1 **At what scales and why does forest structure vary in naturally dynamic boreal**

2 **forests? An analysis of forest landscapes on two continents**

3

4 Niko Kulha[*], Leena Pasanen, Lasse Holmström, Louis De Grandpré, Timo Kuuluvainen, Tuomas

5 Aakala

6

7 N. Kulha, T. Kuuluvainen, T. Aakala

8 Department of Forest Sciences, University of Helsinki. P.O. Box 27, FI-00014 Helsinki, Finland

9

10 L. Pasanen, L. Holmström

11 Research Unit of Mathematical Sciences, University of Oulu. P.O. Box 8000, FI-90014 Oulu,

12 Finland

13

14 L. De Grandpré

15 Canadian Forest Service, Laurentian Forestry Centre. P.O. Box 3800, Sainte-Foy, Quebec GIV

16 4C7, Canada

17

18 [*] Corresponding author.

19 OrcID: 0000-0002-1610-9938

20 Tel. +358405011588

21 E-mail address: niko.kulha@helsinki.fi

22 **Abstract**

23

24 Identifying the scales of variation in forest structures and the underlying processes are fundamental

25 for understanding forest dynamics. Here, we studied these scale-dependencies in forest structure in

26 naturally dynamic boreal forests on two continents. We identified the spatial scales at which forest

27 structures varied, and analyzed how the scales of variation and the underlying drivers differed

28 among the regions and at particular scales.

29

30 We studied three 2 km × 2 km landscapes in northeastern Finland and two in eastern Canada. We

31 estimated canopy cover in contiguous 0.1-ha cells from aerial photographs and used scale-

32 derivative analysis to identify characteristic scales of variation in the canopy cover data. We

33 analyzed the patterns of variation at these scales using Bayesian scale space analysis.

34

35 We identified structural variation at three spatial scales in each landscape. Among landscapes, the

36 largest scale of variation showed greatest variability (20.1 – 321.4 ha), related to topography, soil

37 variability, and long-term disturbance history. Superimposed on this large-scale variation, forest

38 structure varied at similar scales (1.3 – 2.8 ha) in all landscapes. This variation correlated with

39 recent disturbances, soil variability, and topographic position. We also detected intense variation at

40 the smallest scale analyzed (0.1 ha, grain of our data), partly driven by recent disturbances.

41

42 The distinct scales of variation indicated hierarchical structure in the landscapes studied. Except for

43 the large-scale variation, these scales were remarkably similar among the landscapes. This suggests

44 that boreal forests may display characteristic scales of variation that occur somewhat independent of

45 the tree species characteristics or the disturbance regime.

46

47 **Keywords**

48 Forest dynamics, Canopy cover, Aerial photography, Bayesian inference, Eastern Canada, Northern

49 Fennoscandia

50

51 **Manuscript highlights**

52 · We identified distinct scales of hierarchical variation in boreal forest structure

53 · The mid-scale variation occurred at remarkably similar scales among the landscapes

54 · Drivers of the structural variation depended on the observation scale

55 **Introduction**

56

57 The spatial variability of forest structure (e.g., tree sizes, distribution of stems and foliage, dead

58 wood) is the result of multiple factors such as disturbances, succession, topography, and soil

59 properties (Lavoie and others 2007; Gauthier and others 2010; Walker and Johnstone 2014).

60 Knowledge of this structural variation is essential for understanding the processes that drive forest

61 dynamics, habitat variability, and biodiversity (Niemelä and others 1996; Kuuluvainen and others

62 2017), along with nutrient and carbon dynamics (Wickland and Neff 2008; Bradshaw and others

63 2009) in forested landscapes.

64

65 Forest structure varies hierarchically at multiple spatial scales (Kotliar and Wiens 1990;

66 Kuuluvainen and others 1998). However, the scales at which the variation occurs are often only

67 described qualitatively (Angelstam and Kuuluvainen 2004; Bouchard and others 2008; Kuuluvainen

68 and others 2014). The multiscale variation reflects the influence of drivers that shape forest

69 structure at different scales, and their cumulative effects (Elkie and Rempel 2001; Wong and

70 Daniels 2016). Some drivers create variation across multiple spatial scales. For example in the

71 boreal forest, topography and soil properties may create variation at the landscape scale by

72 changing the predisposition of stands to high winds (Ruel and others 1998) and by influencing the

73 tree species composition (Sutinen and others 2002), and at the small, within-stand scales, by

74 influencing the occurrence of suitable regeneration sites (Kuuluvainen and Kalmari 2003; Grenfell

75 and others 2011). Similarly, disturbances such as forest fire may induce variation at the landscape

76 scales (De Grandpré and others 2000; Gauthier and others 2010), while insect outbreaks and wind

77 disturbances typically create variation at stand scales (Kuuluvainen and others 1998; Pham and

78 others 2004). The influence of some other drivers, such as tree-tree competition (Aakala and others

79   2016), or the senescence-related deaths of individual trees (Aakala and others 2009) is limited to

80   within-stand scales.

81

82   Studies on forest structures and dynamics often focus on *a priori*-selected scale, or on the effect of a

83   specific driver. However, as structural variation occurs at multiple scales and results from multiple

84   drivers, a single scale or focus on a specific driver is often insufficient for comprehensive landscape

85   analysis (Habeeb and others 2005; Scholes 2017; Estes and others 2018). Furthermore, the patterns

86   of structural variation and their linkages to the drivers of variation have a fundamental connection

87   with the spatial scale of observation (Wu and Loucks 1995), highlighting that studies on forest

88   structural variability would benefit from methods that do not rely on scales selected *a priori* (Hay

89   and others 2002). Instead, the complex nature of forest ecosystems requires an analysis of patterns

90   in forest structures and the underlying processes in which the scales of observation are reduced to

91   those containing the most salient features (i.e. the characteristic scales of variation; Wu 1999). The

92   identification of such scales is the first step towards understanding the multiscale linkages of

93   ecological patterns and processes (Scholes 2017).

94

95   Here, we studied the scale-dependent variation in boreal forest structure and the factors influencing

96   this variation. We hypothesized that in forest landscapes (1) structural variation occurs at specific,

97   discernible spatial scales, but (2) these discernible scales of variation differ between regions and

98   landscapes, and (3) we can identify different (scale-dependent) drivers of structural variation behind

99   these patterns.

100

101   We tested these hypotheses in five naturally dynamic boreal forest landscapes in two regions,

102   northern Finland and northeastern Quebec, Canada. Using visual interpretation of canopy cover

103   variation on recent aerial photographs calibrated against field measurements, we applied scale-

104   derivative analysis (Pasanen and others 2013) and Bayesian scale space multiresolution analysis

105   (Holmström and others 2011). These methods aim to recognize characteristic scales of forest

106   structural variation, assess the spatial occurrence of structural variation, and identify structurally

107   distinct areas in the study landscapes.

108

109   Material and Methods

110   Study area

111

112   We examined forests in two regions: northeastern Finland (67°44' N, 29°33' E) and the North Shore

113   region in Quebec, Canada (49°38' N, 67°55' W; Fig. S1). In Finland, we examined two landscapes

114   (2 km × 2 km) in Värriö Strict Nature Reserve (Hirvaskangas and Pommituskukkulat), and a third

115   landscape in Maltio Strict Nature Reserve (Hongikkovaara). In Quebec, we studied two landscapes,

116   Lac Dionne and Pistuacanis.

117

118   The studied landscapes are mosaics of forests on mineral soil, waterbodies, and forested and open

119   peatlands. Soils in northeastern Finland consist mostly of undifferentiated glacial tills, with gentle

120   slopes, and low mountain fells with treeless upper slopes. The elevation ranges between 200 and

121   500 meters above sea level (asl). In the North Shore region of Quebec, slopes vary from low to

122   moderate. Undifferentiated glacial tills are common on the gentle slopes and depressions, as are

123   glaciofluvial sand deposits in floors of larger valleys and rocky outcrops on moderate slopes and

124   summits (Robitaille and Saucier 1988). Here, the elevation of the studied region ranges from 300 to

125   500 meters asl. Northern Finland has a subcontinental climate, with an annual mean temperature of

126   +0.9 °C. The climate in the North Shore region is humid, with an annual mean temperature of

127   +0.3 °C (see Supplementary material 1 for details).

128

129   Low tree species diversity is characteristic of both regions. The main tree species in Finnish

130   landscapes are *Pinus sylvestris* (L.), *Picea abies* (L.) Karst, and *Betula pubescens* (Ehrh.). *Picea*

131   *mariana* (Mill.) and *Abies balsamea* (L.) Mill. dominate in Quebecois landscapes. The tree species

132   composition of both regions reflects site productivity and long-term disturbance history

133   (Supplementary material 1).

134

135   **Visual interpretation of canopy cover**

136

137   To quantify forest structural variation at various spatial scales, we first visually interpreted canopy

138   cover from recent aerial photographs in each of the five study landscapes. We used stereopairs of

139   false-color aerial photographs with a pixel size of 0.5 m. Photographs for northern Finland were

140   obtained from the National Land Survey of Finland, and were taken during summers 2011

141   (Hirvaskangas and Pommituskukkulat) and 2010 (Hongikkovaara). Photos for Quebec were

142   obtained from the Ministère des Forêts, de la Faune et des Parcs du Québec, and were taken in

143   2011. We performed the stereointerpretation with EspaCity software (version 11.0.15306.1; Espa

144   Systems Ltd., Espoo, Finland), using a passive 3D monitor.

145

146   During the interpretation, we visually estimated canopy cover in 0.1-ha cells. For this, we placed a

147   square grid of 64×64 cells over each landscape. To reduce bias due to improving interpretation

148   skill, we divided the grids into sixteen parts (256 cells each), and the first author interpreted these

149   sub-grids in randomized order. For each cell, we recorded total canopy cover and the proportion of

150   various tree species. We identified conifers to species level, but did not separate deciduous trees.

151   We estimated canopy cover as the proportion of forest floor covered by the vertical projection of a

152   tree crown. Further, we counted the number of standing and fallen dead trees, which we later used

153   as a measure of recent disturbances (see below). If a cell was not completely within a forest (e.g.,

154   waterbody, open peatland), we excluded it from further analyses. In Pommituskukkulat, we also

155   excluded cells overlapping or bordering a reindeer fence traversing the area.

156

157   **Calibration of and error in the visual interpretation**

158

159   To reduce bias in the visual interpretation and to quantify the interpretation error, we field-sampled

160   randomly selected grid cells, and reconstructed canopy cover for these cells at the year

161   corresponding to the aerial photographs. In Finland, we sampled 16 cells per landscape (as

162   described in Aakala and others 2016). In Quebec, logistical constraints limited the sample size to

163   nine cells per landscape. In each sampled cell, we mapped all living and dead trees with a minimum

164   diameter of 10 cm at 1.3 m height whose crown reached within the cell. We extracted samples for

165   tree-ring width measurements from each tree (see Supplementary material 2 for details). For live

166   trees, we mapped crown projections by measuring 4 – 8 points along the crown dripline. We

167   converted the crown measurements into irregular polygons and used the tree-ring width

168   measurements to reconstruct the crown sizes corresponding to the year the aerial photograph for

169   that landscape was taken. We used species-specific regression models between tree diameter and

170   crown projection area to convert change in tree size to change in crown size (Figs. S2 – S3). We

171   used tree-ring widths to cross-date the year of death for the sampled dead trees, and assumed

172   circular crowns for trees that died between field sampling and the year the aerial photograph was

173   taken. From the reconstructions, we calculated the canopy cover of the sampled cells as the non-

174   overlapping sum of individual crown projections.

175

176   We calibrated the visual interpretation and quantified the interpretation error using regression

177   models between the interpreted and reconstructed canopy covers for Finnish and Quebecois

178   landscapes individually (Figure 1; see Supplementary material 3 for details). We tested the

179   influence of additional variables (tree species proportions, distance from cells to aerial photograph

180   nadirs) for the calibration model in the Finnish landscapes. According to Akaike information

181   criterion for small sample sizes (AICc), the model fit improved when we included the proportion of

182   *P. abies* in the cell as a predictor (Table S1). Hence, we included it in the final calibration model for

183   the Finnish landscapes (Fig. S4). We then compiled the calibrated canopy cover values into raster

184   maps, and used the interpretation error (i.e. the residuals of the calibration model) in Bayesian

185   inference (see below).

186

187   Similar to canopy cover, we calibrated the visual interpretation of the number of snags and logs

188   (minimum diameter 10 cm at 1.3 m height) in each cell with the equivalent dead wood basal area

189   measured in the field (Figs. S5 – S6). Zero snags and logs were interpreted in many grid cells.

190   Hence, the dead wood posterior predictive samples could have had negative draws (negative dead

191   wood basal area). We tested the influence of the negative samples to the results by replacing all the

192   negative draws in the samples with zero. Truncation of the negative values did not affect the

193   interpretation of the results (Supplementary material 3).

194

195

196   **Identification of the scales and spatial patterns of canopy cover variation**

197

198   Our aims were to identify spatial scales of variation for each landscape, and to assess the spatial

199   patterns of this variation at the identified scales. For this, we used Bayesian scale space

200   multiresolution analysis (Holmström and others 2011). The use of this approach on a canopy cover

201   raster map relies on the idea that the raster consists of a sum of components of various spatial

202   scales. Hence, smoothing the raster can reveal features that correspond to a signal at various scales.

203   A low smoothing level maintains all but the smallest-scale variation in the signal, and a high level

204 of smoothing evens out the small-scale details and reveals only locally average behavior in the

205 signal. To extract the relevant scales of variation and study the features at each particular scale

206 separately (as suggested by e.g., O'Neill and others 1986), the scale space multiresolution analysis

207 considers the differences of smooths, where a smooth with a higher smoothing level is subtracted

208 from a smooth with a lower smoothing level. We henceforth call the product of this subtraction

209 (signal at a particular scale) the 'scale-dependent component'.

210

211 The analysis consists of five steps (Fig. 1): 1) calibration of the visual interpretation, 2) scale

212 identification, 3) multiresolution decomposition, 4) credibility assessment, 5) feature size estimation

213 that are next described in more detail.

214

215 In step 1, based on the calibration models described above, we built a Bayesian model for the

216 calibrated canopy covers using the interpreted and field-measured canopy cover (see Supplementary

217 material 3 for details).

218

219 In step 2, the scales of variation are identified. The identification of the spatial scales at which the

220 most salient features in the raster maps occur requires that the smoothing levels are determined

221 carefully. For this, we used an objective approach based on a concept of 'scale-derivative', which

222 refers to the derivative of a signal smooth with respect to the logarithm of the smoothing level

223 (Pasanen and others 2013). The relevant scales are detected based on the locations of local minima

224 of a scale-derivative vector norm. In brief (see Pasanen and others 2013 for full details), consider a

225 signal that consists of a sum of two components of different scales. The location of a local

226 minimum then represents a scale at which the smaller scale component is smoothed out, revealing

227 the larger-scale component not yet affected by smoothing. Hence, the signal including the small-

228 scale variation can be recovered as the difference between the original signal and the smooth

229 corresponding to the local minimum. In general, a smoothing level sequence is defined using such

230 local minima of the scale-derivative norm, and the variations at different scales (i.e. scale-dependent

231 components) are resolved as the differences between the smooths of two consecutive smoothing

232 levels. Henceforth, we call these identified local minima as scale breaks (*sensu* Wu 1999).

233

234 In the context of forest structure, a scale break represents a transition between hierarchical levels of

235 variation. Within a variation level, the first break represents the grain and the second the extent of

236 the particular level. In our analysis, the scale-derivative did not always detect the scale breaks

237 automatically. In such cases, we visually searched the norms for weaker signs of scale breaks such

238 as saddle points or changes in slope. We verified the existence of the identified scales by comparing

239 the scale-derivative norm of the canopy cover (sum of all scale-dependent components) to the scale-

240 derivative norm of permuted canopy cover (Fig. S7). Only the small-scale component could be

241 identified from the permuted data, confirming the existence of the identified characteristic scales of

242 variation.

243

244 In step 3, the canopy cover raster map is decomposed into scale-dependent components. Following

245 the identification of the characteristic scales of variation, we assessed the spatial patterns of

246 variation in canopy cover at the scales in question. We smoothed the canopy cover raster maps

247 based on the identified scale breaks, and produced the scale-dependent components as subtractions

248 of the smooths. The results were maps that depict canopy cover at a location relative to its

249 surroundings, where sizes of the locations and surroundings depend on the smoothing level (i.e.

250 with increased smoothing, larger areas are compared to their surroundings). When extracting the

251 highest smoothing level component, we subtracted the mean of the original image from the highest

252 smooth. We used a Nadaraya-Watson smoother with a Gaussian kernel for the smoothing (e.g.,

253 Wand and Jones 1994). We henceforth refer to these extractions as relative canopy cover maps,

254 where each identified scale and landscape have their own map.

255

256 In step 4, the credibility of the canopy cover variation patterns is assessed. We used Bayesian

257 inference to account for the uncertainty stemming from the calibration models and to distinguish

258 credible variation from the visual interpretation error noise in the relative canopy cover maps. We

259 developed posterior distributions for canopy cover, based on the error in the regression model

260 between interpreted and field-measured canopy cover. We first drew a large sample from this

261 posterior predictive distribution, and approximated the posterior distribution of each relative canopy

262 cover map by applying the difference of smooths operator to each sampled image (see

263 Supplementary material 3 for details). We then identified the credibly positive and negative cells

264 from each relative canopy cover map, using simultaneous inference over all cells by applying the

265 method of highest point-wise probabilities (HPW; Erästö and Holmström 2005; Holmström and

266 others 2011), with a posterior probability threshold of 0.95.

267

268 In step 5, the sizes of the features in the relative canopy cover maps are assessed. To produce

269 quantifiable and comparable information at the characteristic scales of variation, we assessed the

270 sizes of the features detected in each of the relative canopy cover maps as the diameter of the

271 representative circle, an approach similar to Pasanen and others (2018). In short (see Supplementary

272 material 3 for details), for determining the diameter of a representative circular feature on each

273 relative canopy cover map, we used the smoothing level indicated by the maximum in the

274 component's scale-derivative norm and the concept of 'full width at half maximum', often used in

275 medical imaging to represent the size of a feature without clear boundaries (Epstein 2007). We note

276 that the size estimation depended on the locations of the scale breaks, a few of which were manually

277 placed. Hence, we assessed the sensitivity of the size estimation with respect to the scale break

278 locations. The size estimates were fairly insensitive to small changes in the scale break locations.

279

280 **Explanatory variables for canopy cover variation**

281

282 To assess the role of various factors driving forest structural variation at multiple scales, we

283 assessed the relationships between relative canopy cover and recent disturbances, edaphic and

284 topographic factors, and long-term disturbance history.

285

286 For recent disturbances, we assumed that the dead wood quantity in a cell is indicative of recent

287 disturbances in the cell. To analyze the relationship between relative canopy cover variation and

288 recent disturbances, we extracted the scale-dependent features of the dead wood basal area, using

289 the same smoothing levels as with canopy cover (henceforth relative dead wood basal area; Fig.

290 S8). The exact way in which we analyzed the relationship between relative dead wood basal area

291 and relative canopy cover depended on the scale analyzed. At the smallest scale, we examined

292 whether the relative dead wood basal area in a cell differed for cells with negative and positive

293 relative canopy cover. Due to the low number of credible canopy cover cells in Quebecois

294 landscapes, we included an additional 50 cells with the lowest and highest relative canopy cover

295 from both Quebecois landscapes in the comparison (total 158 positive, 64 negative cells in Finnish,

296 and 129 positive, 113 negative cells in Quebecois landscapes). For larger scales, we tested the

297 dependency using local correlation analysis, and assessed the credibility of the correlation in each

298 landscape (cf. Pasanen and Holmström 2017). In this analysis, we calculated Pearson correlation

299 coefficients between the relative dead wood basal area and the relative canopy cover on a moving

300 window. We increased window size along with the increasing smoothing level. The credibilities of

301 the correlations were determined by drawing a large sample from the canopy cover and dead wood

302 posterior probability distributions, using the HPW method with a credibility level of 0.95.

303

304 To assess the role of site productivity and long-term disturbance history as determinants of relative

305 canopy cover, we relied on the predictability of tree species composition as a function of site

306 productivity and/or disturbance history (Supplementary material 1). We compared tree species

307 composition maps to the credible features of the relative canopy cover maps. We utilized

308 independently compiled tree species composition maps for Quebec (Ministère des Forêts, de la

309 Faune et des Parcs du Québec), based on the aerial photointerpretation of an experienced

310 interpreter. We lacked such independent maps for Finland, and therefore used tree species

311 compositions recorded during the visual interpretation of the aerial photographs, calibrated with

312 field measurements (Figs S9−S11). To ensure that the correlation between tree species composition

313 and canopy cover was not the result of including the proportion of *P. abies* in the calibration model

314 for Finnish landscapes, we also performed the calibration without *P. abies* as a predictor, and tested

315 the dependency with this model. The correlations between tree species composition and canopy

316 cover were independent of the used calibration model.

317

318 To assess how topography affects relative canopy cover at various spatial scales, we computed

319 topographic variables from digital elevation models with a spatial resolution of 20 m (National

320 Land Survey Finland, Ministère des Forêts, de la Faune et des Parcs du Québec). Variables tested

321 included elevation (mean elevation of each 0.1-ha cell), slope steepness (cell mean), slope aspect

322 (cell midpoint aspect), and topographic position (cell mean; Jenness and others 2013). If an area is

323 higher than its surroundings, its topographic position index is positive, and vice versa. We defined

324 the index on three scales: between individual cells and between groups of 10 and 20 cells. We

325 computed Spearman's rank correlations between the means of the posterior predictive distributions

326 (each relative canopy cover map) and the topographic variables. If this correlation coefficient was >

327 0.15, we assessed the uncertainty of the correlation by computing correlations between the

328 particular topographic variable and all the 10 000 draws of the posterior predictive distribution, and

329 assessed the mean and the 95% credibility intervals for these correlations.

330

331

332 **Results**

333

334 **Canopy cover and scales of variation**

335

336 Canopy cover in the 0.1-ha cells ranged from 0 to 59% in the Finnish landscapes, with a posterior

337 mean of average over all cells 25% (SD of posterior predictive sample ±8%, 95% prediction

338 interval 18 – 33%) (Fig. 2 a1 – c1). Canopy cover ranged from 3 to 70% in the Quebecois

339 landscapes, with a posterior mean of average over all cells 35% (SD ±13%, 95% prediction interval

340 22 – 48%) (Fig. 2 d1 – e1).

341

342 In the scale-derivative analysis, we identified three scales of forest structural variation in each

343 landscape, which we henceforth call large-, mid-, and small-scale variation (Fig. 3). The analysis

344 automatically identified the scale breaks between mid- and large-scale components. We manually

345 placed the scale breaks between the small- and mid-scale components at the location in which the

346 slope of the scale-derivative norm became less steep, indicating that the small-scale component

347 appeared smoothed out. The permutation test, where we compared the scale-derivative norms for

348 the canopy cover to the scale-derivative norm for permuted canopy cover confirmed the existence

349 of the identified characteristic scales of variation (Fig. S7).

350

351   Feature sizes at the largest scale identified varied among the landscapes. A typical large-scale

352   feature diameter was 2023 m in Hirvaskangas, 696 m in Pommituskukkulat and Hongikkovaara,

353   506 m in Lac Dionne and 1518 m in Pistuacanis. These diameters correspond to an area of 321.4 ha

354   in Hirvaskangas, 38.1 ha in Pommituskukkulat and Hongikkovaara, 20.1 ha in Lac Dionne and

355   181.0 ha in Pistuacanis.

356

357   A typical mid-scale feature diameter was 190 m in each landscape except Hongikkovaara and Lac

358   Dionne, corresponding to a circle area of 2.8 ha. In Hongikkovaara and Lac Dionne, a typical mid-

359   scale feature diameter was 127 m (1.3 ha). The small-scale variation corresponded to the grain size

360   in our data (0.1-ha grid cells, diameter 31.62 m) in each landscape.

361

362   We used the scales identified in the scale-derivative analysis to produce relative canopy cover maps

363   (Fig. 2). In these maps, negative relative canopy cover means low canopy cover in relation to the

364   surroundings, while the opposite is true for positive canopy cover. At the large scale, relative

365   canopy cover ranged from -10 to 10 percentage points in Finnish landscapes and from -13 to 10 in

366   Quebec (Fig. 2 a2 – e2). At the mid scale, relative canopy cover ranged from -13 to 15 percentage

367   points in Finnish landscapes and between -24 and 21 in Quebec (Fig. 2 a4 – e4). At the small scale,

368   relative canopy cover ranged from -15 to 18 in Finnish landscapes and between -26 and 24 in

369   Quebec (Fig. 2 a6 – e6).

370

371   The range of canopy cover values was greatest in Pistuacanis (Fig. 2 e1), which is reflected in the

372   relative canopy cover map intensities (Fig. 2). This intensity difference, visible in the mid- and

373   small-scale components, is also visible as differences in the scale-derivative norms (Fig. 3).

374

375   At the large scale, Hirvaskangas (Fig. 2 a2) and Pistuacanis (Fig. 2 e2) showed two contrasting

376   credible canopy cover areas. We observed several smaller areas of credibly high (low) relative

377   canopy cover in Pommituskukkulat (Fig. 2 b2), Hongikkovaara (Fig. 2 c2), and Lac Dionne (Fig. 2

378   d2). All five landscapes showed a higher number of credibly negative or positive relative canopy

379   cover features at the mid scale than at the small scale, and more credible features were observed in

380   Finnish than in Quebecois landscapes (Fig. 2 a2 – e7). Pommituskukkulat had the most credible

381   patches of all the Finnish landscapes at the mid- and small-scales (Fig. 2 b5, b7). In Quebec,

382   Pistuacanis landscape had the most small- and mid-scale scale credible patches (Fig. 2 e5, e7).

383

384   **Drivers of canopy cover variation**

385

386   *Recent disturbances*

387

388   At mid-scale, average correlations between relative canopy cover and relative dead wood basal area

389   varied from -0.02 to 0.09. However, we observed wide spatial variability in the correlations, from -

390   0.78 to 0.83 (Fig. 4). In the Finnish landscapes, these correlations were credible in the eastern and

391   northwestern parts of Hirvaskangas (Fig. 4f), in the middle, and southeastern part of

392   Pommituskukkulat (Fig. 4g), and in two areas in the middle of Hongikkovaara (Fig. 4h). Several of

393   the mid-scale features correlated credibly with relative dead wood basal area in the Quebecois

394   landscapes (Fig. 4i – j).

395

396   We visually judged which of the credible mid-scale canopy cover patches in Quebec likely resulted

397   from a previous spruce budworm (*Choristoneura fumiferana* (Clem.)) outbreak, based on field

398   observations. In *P. mariana*-dominated Lac Dionne, 10% of the credible negative mid-scale patches

399   occurred at openings that were likely caused by the spruce budworm outbreak. In *A. balsamea-*

400   dominated Pistuacanis, 35% of the negative mid-scale patches were located at these openings. As

401   the variable examined was the canopy cover relative to its surroundings, it is also possible that the

402   loss of canopy cover due to the outbreak results in credibly positive relative canopy cover in the

403   adjacent area. Accordingly, 15% and 30% of the positively deviating patches were next to these

404   openings in Lac Dionne and Pistuacanis, respectively.

405

406   Small-scale relative canopy cover had a connection with relative dead wood basal area (Fig. 5).

407   In both regions, the cells with credibly positive relative canopy cover had a lower posterior

408   median relative dead wood basal area (our surrogate measure for recent disturbances) than the

409   cells with credibly negative relative canopy cover (Fig. 5). Thus, cells with high canopy cover

410   tended to have less dead wood than cells with low canopy cover. However, the relative dead

411   wood amounts did not deviate credibly from zero.

412

413   We did not detect large-scale correlations that would link the relative dead wood basal area (recent

414   disturbances) to relative canopy cover.

415

416   *Site productivity and disturbance history*

417

418   At the large scale, most areas with positive relative canopy cover in the Pommituskukkulat

419   landscape were in areas with a high proportion of deciduous trees (productive sites with shorter

420   time since fire than sites with higher proportion of spruce; Fig. S10-11), whereas the negative

421   relative canopy cover areas were mostly located in *P. abies*-dominated sites (old-growth productive

422   sites). The credible large-scale features in Hirvaskangas and Hongikkovaara occurred independent

423   of tree species composition. Roughly 70% of the areas with positive relative canopy cover in Lac

424   Dionne were dominated by *A. balsamea* and roughly 60% of the areas with negative relative canopy

425   cover by *P. mariana*. The credible large-scale features in Pistuacanis landscape occurred

426   independent of tree species composition.

427

428   The comparison of credible mid-scale canopy cover patches against tree species composition (our

429   surrogate for site productivity and long-term disturbance history, see Supplementary material 1 for

430   details) showed that sites with credible canopy cover features tended to be located in areas where

431   tree species composition changed (Figs. S10-11). This was especially apparent in

432   Pommituskukkulat (roughly 70% of credible mid-scale patches), Hongikkovaara (80%), and Lac

433   Dionne (70%). Particularly the large mid-scale patches with credibly positive relative canopy cover

434   in Pommituskukkulat were located in areas with a high proportion of deciduous trees (productive

435   sites with shorter time since fire). Here, roughly 60% of the negative relative canopy cover areas

436   were on *P. abies*-dominated productive old-growth sites. In Hongikkovaara approximately 60% of

437   the negative patches were on *P. abies*-dominated productive old-growth sites. In Lac Dionne,

438   roughly 80% of the areas with positive relative canopy cover were on *A. balsamea*-dominated sites

439   (productive sites), whereas approximately 60% of the negative relative canopy covers were on *P.*

440   *mariana*-dominated areas (poor sites; Figs. S10-11). In Pistuacanis, the mid-scale relative canopy

441   cover was independent of tree species composition.

442

443   *Topography*

444

445   At the large scale, elevation correlated negatively with relative canopy cover in Hirvaskangas

446   (posterior mean of Spearman's rho (r) -0.89, 95% highest density interval (HDI) -0.90 – -0.87;

447   Table 1), Hongikkovaara (posterior mean of r = -0.34, 95% HDI -0.38 – -0.30), and Pistuacanis

448   (posterior mean of r = -0.54, 95% HDI -0.56 – -0.51). In Pommituskukkulat (posterior mean of r

449   0.21, 95% HDI 0.14 – 0.23) and Lac Dionne (posterior mean of r 0.18, 95% HDI 0.08 – 0.20),

450   elevation correlated positively with relative canopy cover.

451

452   Slope steepness in Hirvaskangas (posterior mean of r -0.29, 95% HDI -0.31 – -0.26) and

453   Pommituskukkulat (posterior mean of r = 0.20, 95% HDI 0.17 – 0.21) and topographic position in

454   Lac Dionne (posterior mean of r = 0.20, 95% HDI 0.16 – 0.23) correlated with large-scale relative

455   canopy cover. Other large-scale correlations with topographic variables were negligible (Table 1).

456

457   The topographic position index at the mid-scale correlated with relative canopy cover only in Lac

458   Dionne (posterior mean of r = 0.19, 95% HDI 0.16 – 0.25). Otherwise, mid-and small-scale relative

459   canopy cover varied independent of topographic variables (Table 1).

460

461   **Discussion**

462

463   Forest structural variation occurred at discernible spatial scales, supporting our first hypothesis.

464   Using the scale-derivative analysis (Pasanen and others 2013), we identified three scales of

465   structural variation in each landscape. These superimposed scales of variation demonstrated the

466   distinctly hierarchical structure in the landscapes, i.e. that small-scale variation occurred within the

467   larger-scale variation levels (Kotliar and Wiens 1990; Elkie and Rempel 2001; Hay and others

468   2002), which is a characteristic feature of ecological systems (O'Neill and others 1986).

469

470   In identifying the scales of variation, we manually placed the scale breaks between the small- and

471   mid-scale, based on the changes in the slope of the scale-derivative norm. In the implemented

472   permutation test, only the small-scale component was identified, confirming the existence of the

473   discerned characteristic scales of variation (Fig. S7). This indicates that the identified scales of

474 variation did not result from a random process. Hence, despite the potential subjectivity involved in

475 placing the scale breaks between the small- and mid-scales, the existence of all the multiresolution

476 components was objectively verified. Further, the identification of scale breaks and multiple scales

477 of variation is consistent with the idea of characteristic scales of variation in naturally dynamic

478 boreal forest landscapes (natural scale steps; Scholes 2017).

479

480 The results only partially supported our second hypothesis concerning the differences of the scales

481 of structural variation. The largest identified variation occurred at scales ranging from 20.1 to 321.4

482 ha, and differed most between the landscapes. In contrast, the second scale of variation (mid scale)

483 was remarkably similar in all five landscapes, ranging from 1.3 to 2.8 ha. Qualitatively, the large-

484 (Angelstam and Kuuluvainen 2004; Bouchard and others 2008) and mid-scales (D'Aoust and others

485 2004; Kuuluvainen and others 2014) of variation have been recognized from boreal forests in both

486 northern Europe and Quebec. Yet, objective quantification of these scales of variation has mostly

487 been lacking.

488

489 Traditionally in landscape ecology, landscape variability is assumed to occur as clearly delineating

490 patches (Kotliar and Wiens 1990). Our results imply that in addition to abrupt changes, gradual

491 structural variability is also typical in naturally dynamic boreal forests. In the Bayesian scale space

492 multiresolution analysis, the variation components are extracted by subtracting successive

493 smoothing levels (Holmström and others 2011). As smoothing suppresses patch edges, features

494 with clear edges also appear as smooth in the mid-scale component. However, if the contrast in the

495 patch edge is strong, the mid-scale patch edges are expected to show as positive and negative bands

496 at the patch edges, visible in the small-scale component. In our results, such banded features were

497 not present. Furthermore, the smoothness of the corresponding patch was visible in the canopy

498   cover maps (Fig. 2 a1 – e1). Hence, our results indicate that structural variability occurs as gradual

499   (but detectable) variability within the forest matrix.

500

501   The smallest scale of variation that we identified equaled the grain of our data, and had high

502   variation intensity. This suggests that intense structural variability in these naturally dynamic boreal

503   forests typically occurs at within-stand scales (< 0.1 ha). Our choice for the grain of the data (i.e.,

504   the interpretation gird) was based on practical reasons for combining fieldwork and the

505   photointerpretation, but also limited our analysis to scales larger than 0.1-ha. However, this scale is

506   similar to the plot size in many (if not most) field-based studies on forest dynamics (Kuuluvainen

507   and Aakala 2011). Hence, the significance of the small-scale variation in the boreal (e.g., Hamel

508   and others 2004; Grenfell and others 2011), as well as the temperate zone (e.g., Runkle and Yetter

509   1987) has clearly been demonstrated. This applies also to both of our study regions (Pham and

510   others 2004; Aakala and others 2016). The low number of credible small-scale relative canopy

511   cover cells in the Quebecois landscapes is the result of their relatively high interpretation error,

512   which is probably related to abundant regeneration following the previous spruce budworm

513   outbreak, which occurred from the 1970s to the mid-1980s (Bouchard and Pothier 2010). In the

514   field measurements, only trees over 10 cm at 1.3 m height were recorded. This distinction was

515   difficult to make in the aerial photointerpretation, leading to high interpretation error.

516

517   Supporting our third hypothesis, we were able to identify the scale-dependent processes creating

518   structural variation in the studied landscapes. The identification of different processes at particular

519   scales also meant that these processes are underlying the patterns at that particular scale (Elkie and

520   Rempel 2001), but also that some of the processes we examined produced patterns at multiple

521   scales. At the largest scale identified, of the topographic variables, elevation had the strongest

522   relationship with structural variation, although the mechanisms differed among the landscapes. In

523   Hirvaskangas, Hongikkovaara, and Pistuacanis landscapes, the relative canopy cover correlated

524   negatively with elevation. This suggests a productivity limitation with increasing elevation, as

525   described earlier in the North Shore region (Boucher and others 2006) and in northeastern Finland

526   (Roiko-Jokela 1980). In both regions, the differences in elevation were modest (100-150 m). Hence,

527   temperature differences are unlikely to explain these findings. Instead, we consider changes in soil

528   nutrient and moisture regimes with topography a more plausible explanation (Seibert and others

529   2007).

530

531   In contrast, elevation and relative canopy cover correlated positively in the Lac Dionne landscape,

532   suggesting increased productivity with increasing elevation. In boreal forests such a relationship has

533   been related to high soil water table levels at low-lying sites (Simard and others 2007), which can

534   cause structural variation even at landscape scales (Kljun and others 2006). In the Lac Dionne

535   landscape, hydric conditions likely locally limit the productivity in low-lying areas, where sparse

536   low productivity *P. mariana*-stands typically dominate (De Grandpré and others 2000).

537

538   Elevation and relative canopy cover also correlated positively in Pommituskukkulat. Here, higher

539   elevation areas were dominated by deciduous trees and had high canopy cover, whereas *P. abies*

540   stands at low elevations had low canopy cover. The areas with a higher deciduous component

541   experienced a fire in 1831 (Aakala 2018), and are separated from the areas with higher dominance

542   of *P. abies* by an open peatland running through the landscape. The peatland probably acted as a

543   fire break, creating variability within the landscape. Hence, the positive correlation between

544   elevation and relative canopy cover in Pommituskukkulat probably reflects the landscape

545   disturbance history more than an elevational effect *per se* (Niklasson and Granström 2000).

546

547   At the mid scale, we detected both negative and positive correlations between relative canopy cover

548   and relative dead wood basal area. The counter-intuitive positive relationship can be explained by

549   variation in soil properties. In the more productive sites, more trees equates to more dead trees,

550   while in less productive sites less trees equates to less dead trees (De Grandpré and others 2000;

551   Kuuluvainen and others 2017).

552

553   The negative relationship between relative canopy cover and relative dead wood basal area

554   demonstrated the role of recent disturbances in shaping forest structure, as tree mortality at these

555   scales caused reduced canopy cover relative to its surroundings. The areas we suspect were related

556   to the previous spruce budworm outbreak and windthrow areas (high numbers of similarly oriented

557   logs) in the Hirvaskangas and Lac Dionne landscapes were visible as negative correlations, and

558   showed that disturbances were responsible for creating variability at these mid scales. The larger

559   number of openings likely caused by the spruce budworm outbreak in *A. balsamea*-dominated

560   Pistuacanis than in *P. mariana*-dominated Lac Dionne is explained by the high susceptibility of *A.*

561   *balsamea* to spruce budworm (Hennigar and others 2008). Spatial variation in boreal forest

562   structures at these patch-scales has previously been linked with disturbances (D'Aoust and others

563   2004; Kuuluvainen and others 2014).

564

565   In addition to disturbances, the credible variation at the mid-scale was related to changes in tree

566   species composition, and to topography in the Lac Dionne landscape. Many of these patches were

567   located in areas where tree species composition changed. This probably reflects changes in edaphic

568   conditions or in time since the last stand-replacing disturbance, as these both affect the tree species

569   composition and tree density (De Grandpré and others 2000; Kuuluvainen and others 2017). The

570   relationship between the topographic position and the mid-scale relative canopy cover in Lac

571   Dionne is likely a result of the same process as observed at the large-scale, i.e. low topographic

572   positions associated with paludification and consequent low relative canopy cover (Lavoie and

573   others 2007; Simard and others 2007).

574

575   We identified tree species composition, long-term disturbance history and recent disturbances as the

576   most important drivers of mid-scale forest structural variation in both regions. However, these

577   factors are related to soil characteristics, which influence the tree species composition (Rowe 1972;

578   Sutinen and others 2002), and the occurrence of fires (Wallenius and others 2004; Mansuy and

579   others 2010) in both regions. Tree mortality from the spruce budworm outbreaks that we identified

580   as a cause for some of the mid-scale patches in the Quebecois landscapes is to a large extent

581   influenced by the tree species composition, and concentrates especially on the *A. balsamea*-

582   dominated stands (D'Aoust and others 2004; Hennigar and others 2008). Hence, although not

583   directly measured here, it seems likely that the variability in soil characteristics creates patch-scale

584   forest structural variation, corresponding to what we observed in this study.

585

586   At the small scale (0.1 ha, the grain of our data), we discovered a relationship between forest

587   structural variation and recent disturbances. Earlier studies have attributed this type of 'stand-scale'

588   variation to tree mortality (Kuuluvainen and others 1998; Aakala and others 2007), which creates

589   structural variation especially in patches smaller than 100 m² (Pham and others 2004). However,

590   this small-scale variability also results from a number of other processes, including the occurrence

591   of regeneration microsites (Grenfell and others 2011), edaphic differences (Hamel and others 2004),

592   and tree interactions (Aakala and others 2016).

593

594   Similar to the grain of our data that excluded the within-stand variability from our analyses, it is

595   evident that some relevant large-scale variability occurred at scales beyond the extent of the study.

596   Most obviously, stand-replacing fires in Quebec cause variability at larger scales than we assessed

597 (De Grandpré and others 2000), and for example, the Lac Dionne landscape is completely within a

598 forest fire area dated to 1810 (Bouchard and others 2008). From a methodological perspective,

599 although we argue that avoiding the selection of study scales *a priori* is a useful approach, the

600 spatial extent and grain still obviously impose limitations on the scales that can be identified and

601 analyzed (Estes and others 2018). Here, the practical limitations related to the calibration data

602 limited the extent, but future work could benefit from the increasing availability of data that is less

603 dependent on well-distributed field plots, such as light detection and ranging (LiDAR) data.

604 However, especially in Finnish landscapes the extent is at the same time limited by the generally

605 small size of the reserves in which natural forest dynamics can be studied.

606

607 Earlier studies have attempted to describe landscape variability over multiple scales using, for

608 instance, scale space theory with blob-feature detection in the hierarchy theory context (Hay and

609 others 2002; Hay 2014), or scalograms that visualize how landscape metrics respond to changing

610 grain and extent (Zhang and Li 2013). The advantage of our approach is that the scale-derivative

611 analysis identifies the characteristic scales of variation uniformly over the entire landscape and

612 extracts the hierarchical components in a mathematically well-defined manner (Pasanen and others

613 2013), using a custom-built metric (cf. Zhang and Li 2013). Thus, it can be widely applied to

614 explore multiscale variability in any raster-form data. The scale space analysis with Bayesian

615 inference (Holmström and others 2011) allows identifying structures at the characteristic scales of

616 variation so that the error associated with the production of the raster data is incorporated in the

617 feature detection. Hence, the credibility of the variability can be assessed whenever the associated

618 error can be quantified.

619

620 That the scale-derivative analysis did not automatically identify all the scale breaks suggests

621 difficulties in the feature extraction due to which information close to a scale break may have been

622 displaced to wrong hierarchical level. It is obvious that the scale breaks may not always produce a

623 local minimum in the norm, and instead weaker signs, such as saddle points or slope changes,

624 should also be inspected as possible scale breaks. The ability of the scale-derivative analysis to

625 separate scale-dependent components automatically depends on the size difference of the features

626 within the components. The smaller the difference, the more difficult the extraction. Large feature

627 size variation within a component and a large intensity difference between successive scale-

628 dependent components can also hamper feature extraction (Pasanen and others 2013). The

629 difficulties in scale break identification represent a typical situation where vague scale level

630 boundaries prove hard to detect (Scholes 2017). We also note that while placing the scale break

631 points manually we introduced subjectivity in the scale identification process. However, small

632 changes in the scale break locations did not cause notable changes in the size estimates and hence

633 our analyses appear robust to this subjectivity.

634

635 The presence of the scale-dependent components, and the occurrence of credible canopy cover

636 features in each extracted scale-dependent component supported the notion of hierarchically

637 structured landscapes, i.e. that there were characteristic scales of variation that contain the most

638 salient structural features (the near-decomposability in the hierarchy theory; O'Neill and others

639 1986). Further, we identified different factors underlying the structural variation at particular scales

640 that is similarly expected from hierarchically structured landscapes (Wu and Loucks 1995; Wu

641 1999). Related to these processes, the hierarchy theory suggests that at large scales variability

642 would be driven by processes changing slowly in time (e.g., topography), whereas at small scales

643 the driving processes occur abruptly (e.g., disturbances) (O'Neill and others 1986; Wu 1999). The

644 occurrence of small-scale disturbances and stand-replacing fires indicates that abrupt processes

645 influence forest structure at local scales, as well as at scales beyond the extent of our study. In

646 contrast, the influence of slowly changing processes was limited to large scales.

647

Conclusions

649

650 Our analyses showed that hierarchical structural variation can be discerned from naturally dynamic

651 boreal forest landscapes without relying on the delineation of distinct patches or on *a priori* selected

652 scales. Further, these scale-dependent variations are linked to a number of different processes that

653 partly crossed spatial scales (i.e. same processes created structural variation at multiple scales).

654 Except for the largest scale variation that was related to landscape-specific topography and the

655 large-scale fires typical in the North American boreal forests, the detected similarity in spatial

656 scales of variation among landscapes suggests that boreal forests may display characteristic scales

657 of variation that are somewhat independent of the dominant tree species or disturbance regime of a

658 landscape.

659

Acknowledgements

661

669

Data availability statement

671

672 Calibration data, and the calibrated raster maps of canopy cover produced in this study will be made

673 available in Figshare at DOI:xxx/xxx upon acceptance.

674

675 **References**

676

677 Aakala T. 2018. Forest fire histories and tree age structures in Värriö and Maltio Strict Nature

678 Reserves, northern Finland. Boreal Environmental Research, in press.

679 Aakala T, Kuuluvainen T, De Grandpré L, Gauthier S. 2007. Trees dying standing in the

680 northeastern boreal old-growth forests of Québec: spatial patterns, rates and temporal variation.

681 Canadian Journal of Forest Research 37: 50-61.

682 Aakala T, Kuuluvainen T, Wallenius T, Kauhanen H. 2009. Contrasting patterns of tree mortality in

683 late-successional *Picea abies* stands in two areas in northern Fennoscandia. Journal of Vegetation

684 Science 20: 1016–1026.

685 Aakala T, Shimatani K, Abe T, Kubota Y, Kuuluvainen T. 2016. Crown asymmetry in high latitude

686 forests: disentangling the directional effects of tree competition and solar radiation. Oikos 125:

687 1035-1043.

688 Angelstam P, Kuuluvainen T. 2004. Boreal forest disturbance regimes, successional dynamics and

689 landscape structures: a European perspective. Ecological Bulletins 51: 117-136.

690 Bouchard M, Pothier D. 2010. Spatiotemporal variability in tree and stand mortality caused by

691 spruce budworm outbreaks in eastern Quebec. Canadian Journal of Forest Research 40: 86-94.

692 Bouchard M, Pothier D, Gauthier S. 2008. Fire return intervals and tree species succession in the

693 North Shore region of eastern Quebec. Canadian Journal of Forest Research 38: 1621-1633.

694 Boucher D, Gauthier S, De Grandpré L. 2006. Structural changes in coniferous stands along a

695 chronosequence and a productivity gradient in the northeastern boreal forest of Québec.

696 Ecoscience 13: 172-180.

697   Bradshaw CJA, Warkentin IG, Sodhi NS. 2009. Urgent preservation of boreal carbon stocks and

698   biodiversity. Trends in Ecology & Evolution 24: 541-548.

699   D'Aoust V, Kneeshaw D, Bergeron Y. 2004. Characterization of canopy openness before and after

700   a spruce budworm outbreak in the southern boreal forest. Canadian Journal of Forest Research 34:

701   339-352.

702   De Grandpré L, Morissette J, Gauthier S. 2000. Long-term post-fire changes in the northeastern

703   boreal forest of Québec. Journal of Vegetation Science 11: 791-800.

704   Elkie PC, Rempel RS. 2001. Detecting scales of pattern in boreal forest landscapes. Forest Ecology

705   and Management 147: 253-261.

706   Epstein CL. 2007. Introduction to the mathematics of medical imaging. Society for Industrial and

707   Applied Mathematics. 84p.

708   Erästö P, Holmström L. 2005. Bayesian multiscale smoothing for making inferences about features

709   in scatterplots. Journal of Computational and Graphical Statistics 14: 569-589.

710   Estes L, Elsen PR, Treuer T, Ahmed L, Caylor K, Chang J, Choi JJ, Ellis EC. 2018. The spatial and

711   termporal domains of modern ecology. Nature Ecology & Evolution 2: 819-826.

712   Gauthier S, Boucher D, Morissette J, De Grandpré L. 2010. Fifty-seven years of composition

713   change in the eastern boreal forest of Canada. Journal of Vegetation Science 21: 772-785.

714   Grenfell R, Aakala T, Kuuluvainen T. 2011. Microsite occupancy and the spatial structure of

715   understorey regeneration in three late-successional Norway spruce forests in Northern Europe.

716   Silva Fennica 45: 1093-1110.

717   Habeeb RL, Trebilco J, Wotherspoon S, Johnson CR. 2005. Determining natural scales of

718   ecological systems. Ecological Monographs 75: 467-487.

719   Hamel B, Bélanger N, Paré D. 2004. Productivity of black spruce and Jack pine stands in Quebec as

720   related to climate, site biological features and soil properties. Forest Ecology and Management

721   191: 239-251.

722 Hay GJ, Dubé P, Bouchard A, Marceau DJ. 2002. A scale-space primer for exploring and

723   quantifying complex landscapes. Ecological Modelling 153: 27-49.

724 Hay GJ. 2014. Visualizing scale-domain manifolds: a multiscale geo-object-based approach. Weng

725   JF, Weng Q, editors. Scale issues in remote sensing. John Wiley & Sons, Incorporated. 141-169.

726 Hennigar CR, MacLean DA, Quiring DT, Kershaw JA Jr. 2008. Differences in spruce budworm

727   defoliation among balsam fir and white, red, and black spruce. Forest Science 54: 158-166.

728 Holmström L, Pasanen L, Furrer R, Sain SR. 2011. Scale space multiresolution analysis of random

729   signals. Computational Statistics & Data Analysis 55: 2840-2855.

730 Jenness J, Brost B, Beier P. 2013. Land facet corridor designer: Topographic position index tools.

731   http://www.jennessent.com/arcgis/land_facets.htm. Accessed 10 October 2017.

732 Kljun N, Black TA, Griffis TJ, Barr AG, Gaumont-Guay D, Morgenstern K, McCaughey JH, Nesic

733   Z. 2006. Response of net ecosystem productivity of three boreal forest stands to drought.

734   Ecosystems 9: 1128-1144.

735 Kotliar NB, Wiens JA. 1990. Multiple scales of patchiness and patch structure: a hierarchical

736   framework for the study of heterogeneity. Oikos 59: 253-260.

737 Kuuluvainen T, Kalmari R. 2003. Regeneration microsites of *Picea abies* seedlings in a windthrow

738   area of a boreal old-growth forest in southern Finland. Annales Botanici Fennici 40: 401-413.

739 Kuuluvainen T, Aakala T. 2011. Natural forest dynamics in boreal Fennoscandia: a review and a

740   classification. Silva Fennica 45: 823-841.

741 Kuuluvainen T, Syrjänen K, Kalliola R. 1998. Structure of a pristine *Picea abies* forest in

742   Northeastern Europe. Journal of Vegetation Science 9: 563-574.

743 Kuuluvainen T, Wallenius TH, Kauhanen H, Aakala T, Mikkola K, Demidova N, Ogibin B. 2014.

744   Episodic, patchy disturbances characterize an old-growth *Picea abies* dominated forest landscape

745   in northeastern Europe. Forest Ecology and Management 320: 96-103.

746 Kuuluvainen T, Hofgaard A, Aakala T, Jonsson BG. 2017. North Fennoscandian mountain forests:

747   History, composition, disturbance dynamics and the unpredictable future. Forest Ecology and

748   Management 385: 140-149.

749 Lavoie M, Harper K, Paré D, Bergeron Y. 2007. Spatial pattern in the organic layer and tree

750   growth: A case study from regenerating Picea mariana stands prone to paludification. Journal of

751   Vegetation Science 18: 213-222.

752 Mansuy N, Gauthier S, Robitaille A, Bergeron Y. 2010. The effects of surficial deposit-drainage

753   combinations on spatial variations of fire cycles in the boreal forest of eastern Canada.

754   International Journal of Wildland Fire 19: 1083-1098.

755 Niemelä J, Haila Y, Punttila P. 1996. The importance of small-scale heterogeneity in boreal forests:

756   variation in diversity in forest-floor invertebrates across the succession gradient. Ecography 19:

757   352-368.

758 Niklasson M, Granström A. 2000. Numbers and sizes of long-term spatially explicit fire history in a

759   Swedish boreal landscape. Ecology 81: 1484-1499.

760 O'Neill RV, DeAngelis DL, Waide JB, Allen THF. 1986. A Hierarchical concept of ecosystems.

761   Princeton Univ. Press. 253p.

762 Pasanen L, Aakala T, Holmström L. 2018. A scale space approach for estimating the characteristic

763   feature sizes in hierarchical signals. Stat, in press.

764 Pasanen L, Launonen I, Holmström L. 2013. A scale space multiresolution method for extraction of

765   time series features. Stat 2: 273-291.

766 Pasanen L, Holmström L. 2017. Scale space multiresolution correlation analysis for time series

767   data. Computational Statistics 32: 197-218.

768 Pham AT, De Grandpré L, Gauthier S, Bergeron Y. 2004. Gap dynamics and replacement patterns

769   in gaps of the northeastern boreal forest of Quebec. Canadian Journal of Forest Research 34: 353-

770   364.

771   Robitaille A, Saucier J-P. 1998. Paysages régionaux du Québec méridional. Les Publications du

772   Québec. Sainte-Foy, CA [In French].

773   Roiko-Jokela P. 1980. Maaston korkeus puuntuotantoon vaikuttavana tekijänä Pohjois-Suomessa.

774   Folia Forestalia 452: 1-30 [In Finnish with English summary].

775   Rowe JS. 1972. Forest regions of Canada. Environment Canada, Ottawa.

776   Ruel J-C, Pin D, Cooper K. 1998. Effect of topography on wind behaviour in a complex terrain.

777   Forestry 71: 261-265.

778   Runkle JR, Yetter TC. 1987. Treefalls revisited: gap dynamics in the Southern Appalachians.

779   Ecology 68: 417-424.

780   Scholes RJ. 2017. Taking the mumbo out of the jumbo: progress towards a robust basis for

781   ecological scaling. Ecosystems 20: 4-13.

782   Seibert J, Stendahl J, Sørensen R. 2007. Topographical influences on soil properties in boreal

783   forests. Geoderma 141: 139-148.

784   Simard M, Lecomte N, Bergeron Y, Bernier PY, Paré D. 2007. Forest productivity decline caused

785   by successional paludification of boreal soils. Ecological Applications 17: 1619-1637.

786   Sutinen R, Teirilä A, Pänttäjä M, Sutinen M-L. 2002. Distribution and diversity of tree species with

787   respect to soil electrical characteristics in Finnish Lapland. Canadian Journal of Forest Research

788   32: 1158-1170.

789   Walker X, Johnstone JF. 2014. Widespread negative correlations between black spruce growth and

790   temperature across topographic moisture gradients in the boreal forest. Environmental Research

791   Letters 9, https://doi.org/10.1088/1748-9326/9/6/064016.

792   Wallenius TH, Kuuluvainen T, Vanha-Majamaa I. 2004. Fire history in relation to site type and

793   vegetation in Vienansalo wilderness in eastern Fennoscandia, Russia. Canadian Journal of Forest

794   Research 34: 1400-1409.

795   Wand MP, Jones MC. 1994. Kernel smoothing. Chapman and Hall/CRC. 224p.

796   Wickland KP, Neff JC. 2008. Decomposition of soil organic matter from boreal black spruce forest:

797   environmental and chemical controls. Biogeochemistry 87: 29-47.

798   Wong CM, Daniels LD. 2016. Novel forest decline triggered by multiple interactions among

799   climate, an introduced pathogen and bark beetles. Global Change Biology 23: 1926-1941.

800   Wu J. 1999. Hierarchy and scaling: extrapolating information along a scaling ladder. Canadian

801   Journal of Remote Sensing 25: 367-380.

802   Wu J, Loucks OL. 1995. From balance of nature to hierarchical patch dynamics: a paradigm shift

803   in ecology. The Quarterly Review of Biology 70: 439-466.

804   Zhang N, Li H. 2013. Sensitivity and effectiveness and of landscape metric scalograms in

805   determining the characteristic scale of a hierarchically structured landscape. Landscape Ecology

806   28: 343-363.

807 **Table**

808

809 **Table 1.** Spearman's rank correlation coefficients between the relative canopy covers at the

810 detected scales (SS = small-scale, MS = mid-scale, LS = large-scale) and the topographic variables

811 for the 0.1-ha cells.

	Hirvaskangas			Pommitus-kukkulat			Hongikkovaara			Lac Dionne			Pistuacanis		
	SS	MS	LS	SS	MS	LS	SS	MS	LS	SS	MS	LS	SS	MS	LS
Elevation	0.00	-0.10	-0.89	0.01	0.06	0.21	0.01	-0.01	-0.34	0.00	-0.01	0.18	0.00	-0.06	-0.54
Slope steepness	-0.01	-0.07	-0.29	0.01	0.09	0.20	0.02	0.04	-0.07	0.01	-0.02	-0.09	0.01	-0.02	0.12
Slope aspect	0.01	0.12	-0.07	0.00	0.02	-0.11	-0.01	-0.03	0.03	0.00	-0.02	-0.04	0.01	0.02	-0.04
TPI	0.01	0.01	-0.05	0.01	0.07	0.09	0.03	0.09	-0.08	-0.01	0.19	0.20	0.01	-0.01	0.11

812

813

814   **Figures**

815
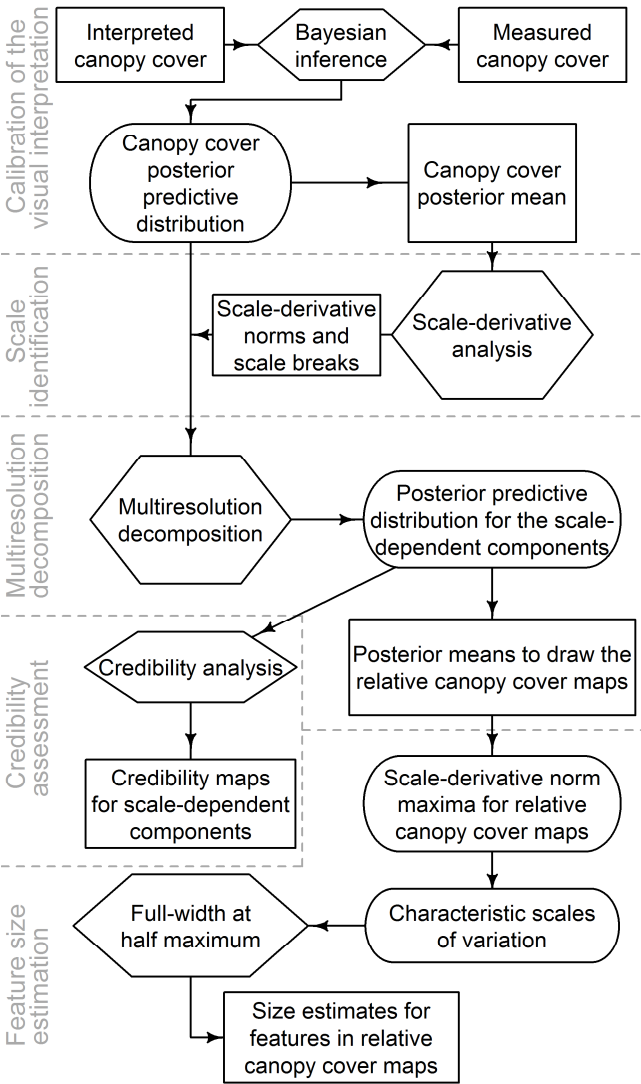
Figure 1. The analysis workflow. The rectangles represent input and output data, the hexagons are

analyses, and the rounded rectangles transitional stage data.
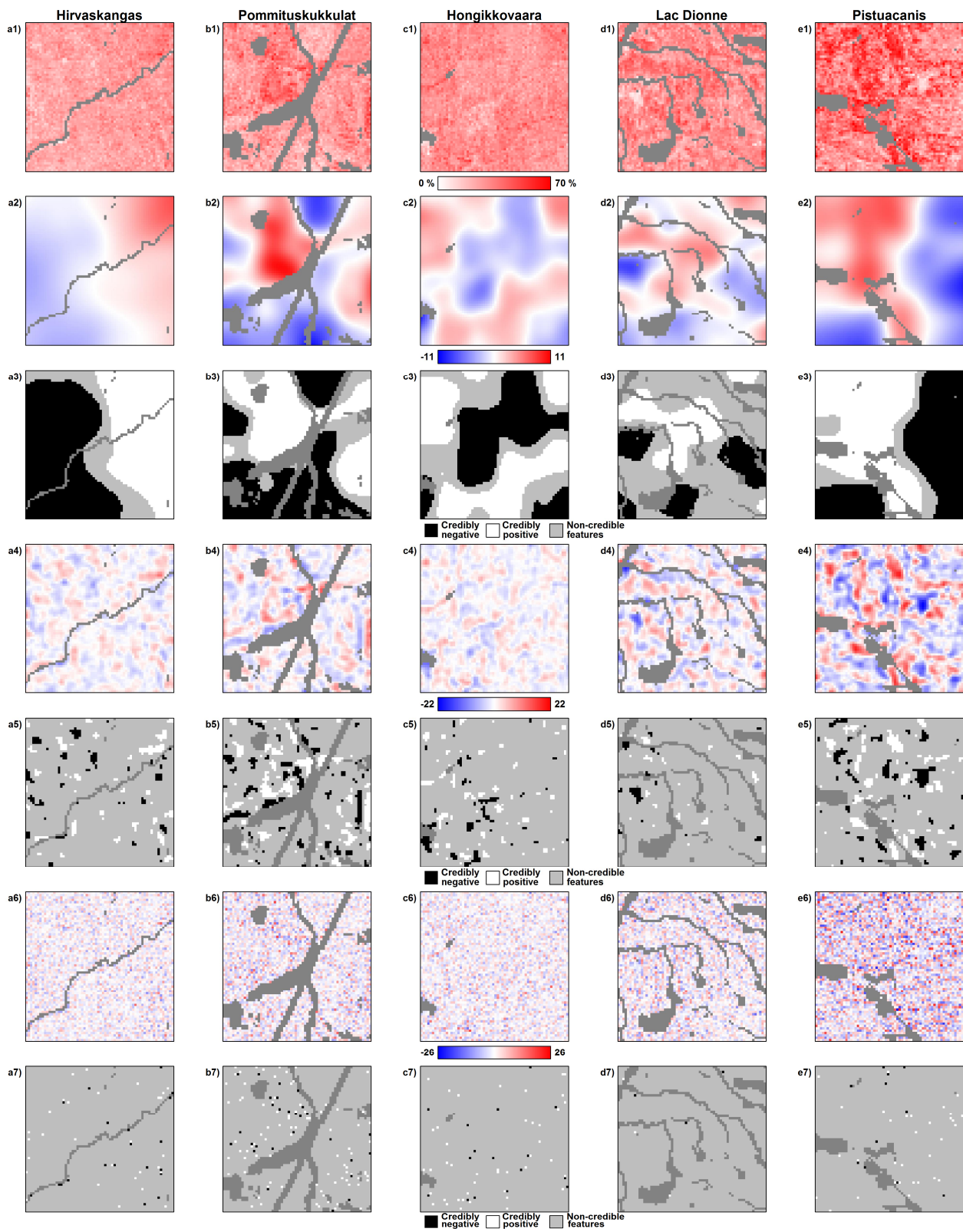
Figure 2. Canopy cover maps of the study landscapes, canopy cover in the 0.1-ha cells (a1 – e1). The large-scale relative canopy cover maps (a2 – e2) and their credibilities (a3 – e3), the mid-scale relative canopy cover maps (a4 – e4) and their credibilities (a5 – e5), and the small-scale relative

822   canopy cover maps (a6 – e6) and their credibilities (a7 – e7). Dark gray areas are nonforest cells,

823   i.e. lakes, streams, open peatlands, and a reindeer fence and its surroundings in the

824   Pommituskukkulat landscape.

825
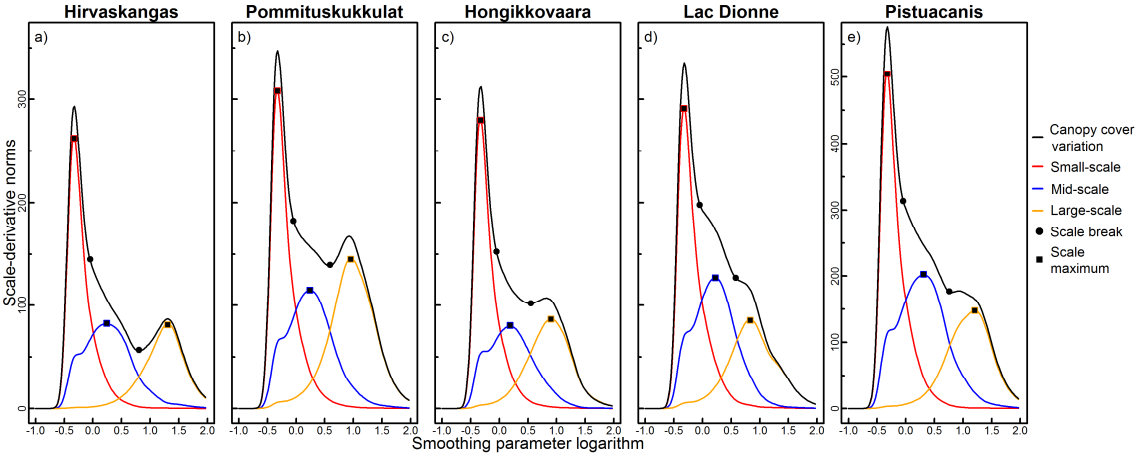
826   **Figure 3.** The scale-derivative norms as a function of the smoothing parameter logarithm. The

827   colored lines show individual components. The points represent the component scale breaks and the

828   squares depict the components' local maxima. *N.B.* the ten-raised smoothing parameter values and

829   the different y-axis scale in the Pistuacanis landscape.

830
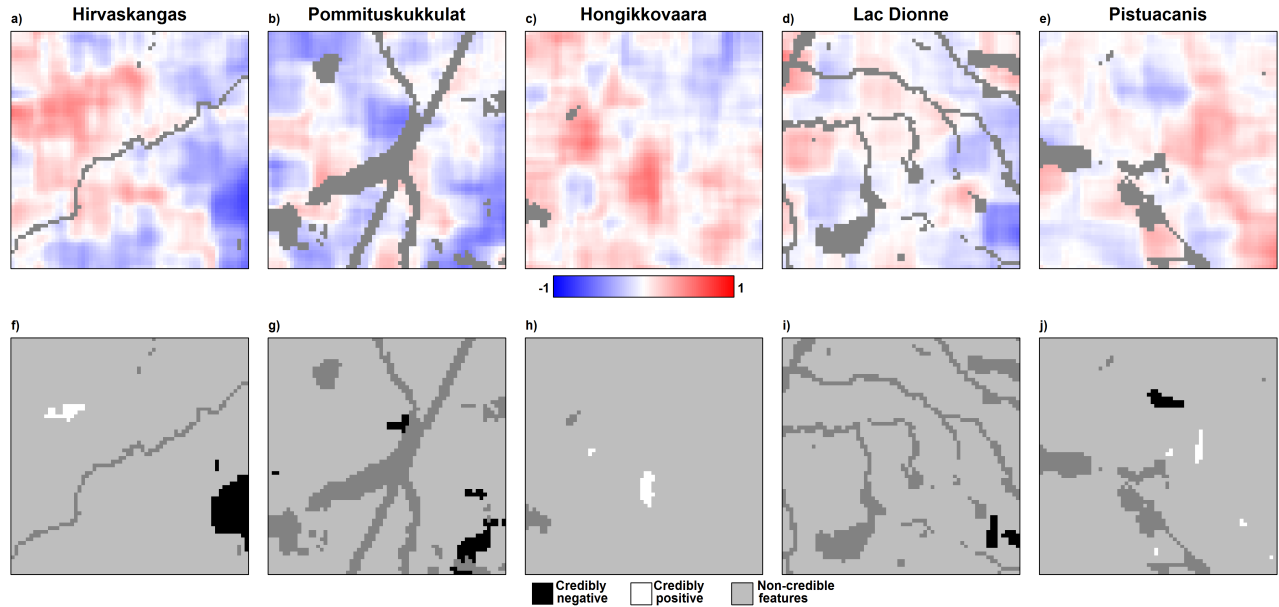
831   **Figure 4.** Local Pearson correlations at the mid scale between relative canopy cover and relative

832   dead wood basal area (posterior mean values, a – e), and their credibilities (f – j). Dark gray cells

833   are non-forested.

834
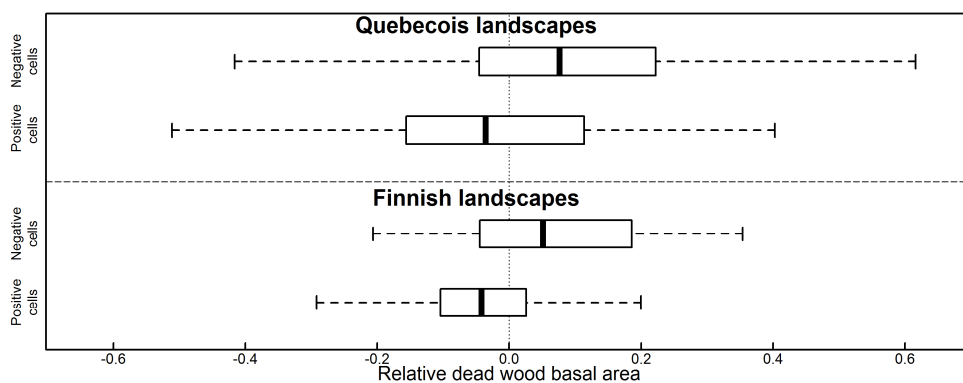
Figure 5. The posterior distributions of the relative dead wood basal area medians in the small-scale

cells with credible relative canopy cover. The distributions consist of 158 positive and 64 negative

cells in the Finnish landscapes and 129 negative and 113 positive cells in the Quebecois landscapes.

838
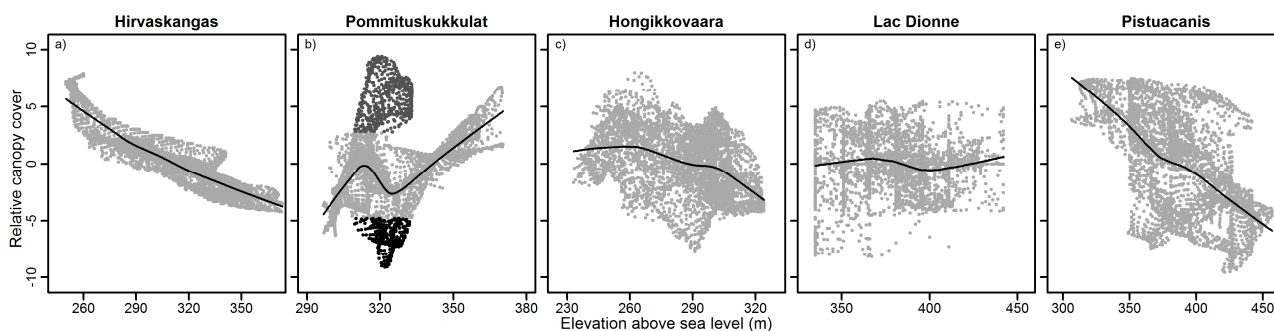
Figure 6. Large-scale relative canopy cover in relation to elevation in the studied landscapes,

illustrated with a lowess regression. Pommituskukkulat (b) landscape has areas that clearly deviate

from the main pattern. Here, the dark gray dots represent a birch-dominated area, and the black dots

represent a hilltop spruce-dominated area. The light gray dots form the main pattern.

1 **Supplementary material for: At what scales and why does forest structure vary**

2 **in naturally dynamic boreal forests? An analysis of forest landscapes on two**

3 **continents**

4

5 Kulha N, Pasanen L, Holmström L, De Grandpré L, Kuuluvainen T, Aakala T

6

7 **Supplementary material 1. Study area characteristics, succession, and**

8 **disturbance history**

9

10 We studied unmanaged boreal forests in two regions: northeastern Finland and the North Shore

11 region in Quebec, Canada (Fig. S1). The mean annual temperature in the study region of

12 northeastern Finland is -0.9 °C. The mean temperatures for the coldest (January) and warmest (July)

13 months are -12.7 °C and +13.1 °C, respectively. The average annual precipitation sum is 570 mm.

14 The mean annual temperature in the North Shore region is +0.3 °C. The mean temperatures for the

15 coldest (January) and warmest (July) months are -17.5 °C and +14.2 °C, respectively. Average

16 annual precipitation is 1100 mm (All climate data are averages from years 1970–2000; Fick and

17 Hijmans 2017).

18

19 Of the individual landscapes, Hirvaskangas is mostly comprised of pure *Pinus sylvestris* (L.) stands

20 (proportion of *P. sylvestris* >75 %). *Picea abies* (L.) Karst. and *Betula pubescens* (Ehrh.) dominate

21 the Pommituskukkulat landscape. In Hongikkovaara, pure *P. sylvestris* stands and mixed *P.*

22 *sylvestris*/*P. abies* stands prevail. *Picea mariana* (Mill.) dominates the Lac Dionne landscape and

23 *Abies balsamea* (L.) Mill. the Pistuacanis landscape. Tree species composition reflects site

24 productivity and long-term disturbance history in both study regions. In Finland, *P. sylvestris*

25 usually dominates low-productivity xeric sites (*sensu* Cajander 1949), independent of successional

26 state. More productive mesic sites usually follow a successional change from *Betula* spp.

27 dominance early in the succession to *P. abies* dominance in the late-successional state (Sirén 1955).

28 In long-term fire absence, *P. abies* increases its share in the initially *P. sylvestris*-dominated sub-

29 xeric sites. In Quebec, *P. mariana* often forms nearly pure stands, while *A. balsamea* may occur as

30 a co-dominant in the more productive sites, or may form monospecific stands (De Grandpré and

31 others 2000). In *A. balsamea*-dominated stands, *Picea glauca* (Moench) Voss often occurs as a co-

32 dominant species.

33

34 Disturbance regimes differ greatly between the studied regions. Similar to northern European boreal

35 forests in general, forest fires were common in the Finnish study region prior to the 20th century,

36 especially surface fires in the xeric *P. sylvestris*-dominated forests (Kuuluvainen and Aakala 2011).

37 In 1831, most of Hirvaskangas and roughly 30% of the nearby Pommituskukkulat landscape

38 burned. This is visible as a "cohort" age structure in the *P. sylvestris* -dominated areas, and as a high

39 proportion of post-fire *B. pubescens* in the mesic parts of the landscape (Aakala, accepted

40 manuscript). The last larger fire in Hongikkovaara occurred in 1777, visible in the age structure,

41 which is similar to Hirvaskangas. In the absence of fire, stand dynamics are driven by small-scale

42 mortality of individual trees or small tree groups (i.e. gap dynamics), punctuated infrequently by

43 storms that may fell trees over larger areas. Additionally, reindeer herding influences Finnish

44 landscapes, and light selection felling connected with reindeer herding has occurred in

45 Hirvaskangas and Pommituskukkulat.

46

47 In the Quebec study region, forests experience periodic spruce budworm *Choristoneura fumiferana*

48 (Clem.) outbreaks, to which *A. balsamea* is especially vulnerable (Bouchard and others 2005).

49 There is an ongoing outbreak in the North Shore region that began ca. 2006 (Bognounou and others

50 2017). The previous severe outbreak occurred from the 1970s to the mid-1980s (Bouchard and

51 Pothier 2010). Between outbreaks, gap dynamics drive the old-growth stands (Pham and others

52 2004). Based on fire maps by Bouchard and others (2008) for the last 200 years, the Lac Dionne

53 landscape burnt in 1810. The Pistuacanis landscape appears to have avoided fires during the last
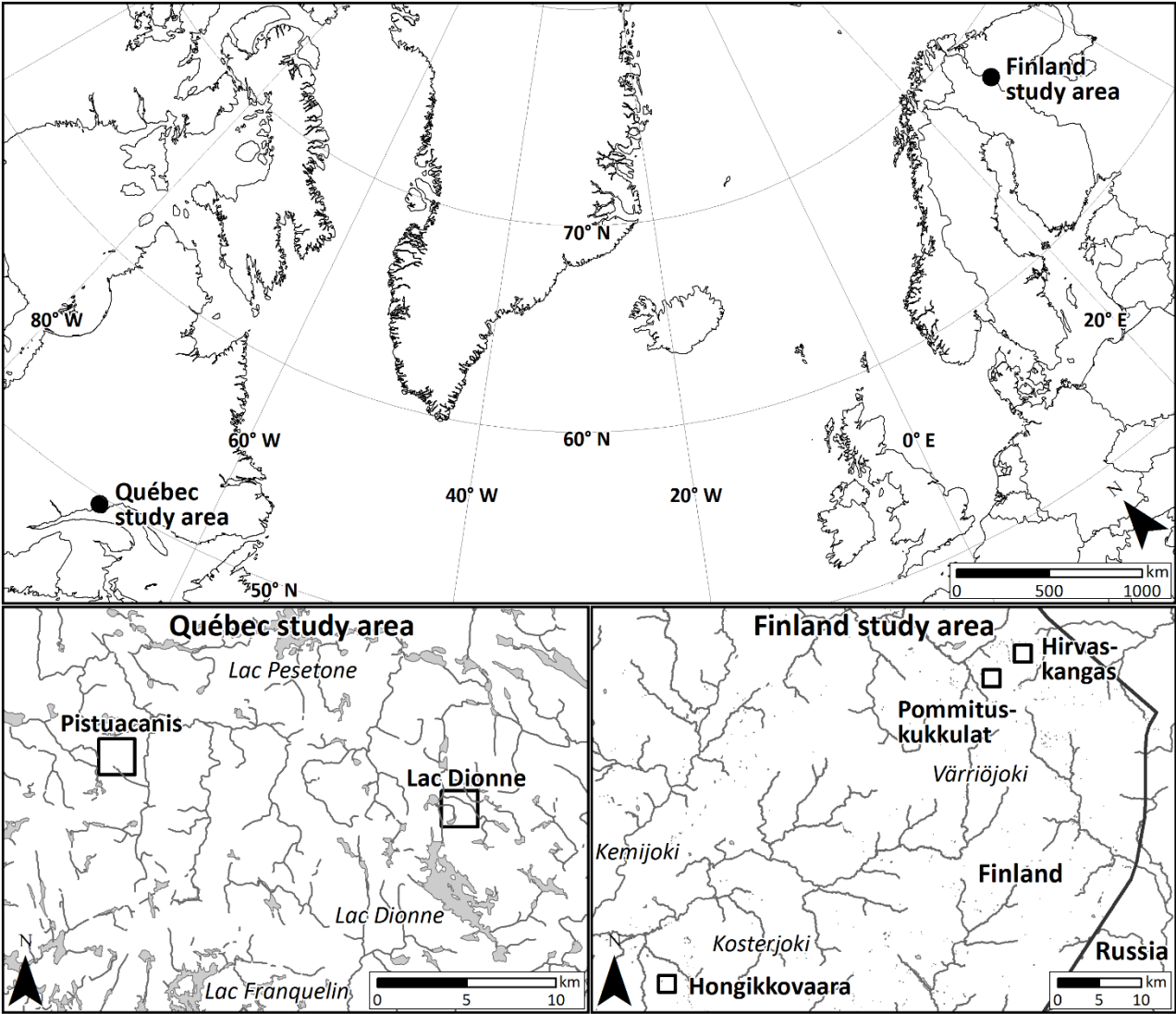
54 200 years.

55

57 **Figure S1.** Study area locations.

58

59 **References**

60

61 Aakala T. 2017. Forest fire histories and tree age structures in Värriö and Maltio Strict Nature

62   Reserves, northern Finland. Boreal Environ Research, accepted manuscript.

63 Bognounou F, De Grandpré L, Pureswaran DS, Kneeshaw D. 2017. Temporal variation in plant

64   neighborhood effects on the defoliation of primary and secondary hosts by an insect pest.

65   Ecosphere 8(3): e01759. DOI: 10.1002/ecs2.1759.

66 Bouchard M, Pothier D. 2010. Spatiotemporal variability in tree and stand mortality caused by

67   spruce budworm outbreaks in eastern Quebec. Canadian Journal of Forest Research 40: 86-94.

68 Bouchard M, Kneeshaw D, Bergeron Y. 2005. Mortality and stand renewal patterns following the

69   last spruce budworm outbreak in mixed forests of western Quebec. Forest Ecology and

70   Management 204: 297-313.

71 Bouchard M, Pothier D, Gauthier S. 2008. Fire return intervals and tree species succession in the

72   North Shore region of eastern Quebec. Canadian Journal of Forest Research 38: 1621-1633.

73 Cajander AK. 1949. Forest types and their significance. Acta Forestalia Fennica 56: 1-71.

74 De Grandpré L, Morissette J, Gauthier S. 2000. Long-term post-fire changes in the northeastern

75   boreal forest of Quebec. Journal of Vegetation Science 11: 791-800.

76 Fick SE, Hijmans RJ. 2017. Worldclim 2: New 1-km spatial resolution climate surfaces for global

77   land areas. International Journal of Climatology 37: 4302-4315.

78 Kuuluvainen T, Aakala T. 2011. Natural forest dynamics in boreal Fennoscandia: a review and

79   classification. Silva Fennica 45: 823-841.

80 Pham AT, De Grandpré L, Gauthier S, Bergeron Y. 2004. Gap dynamics and replacement patterns

81   in gaps of the northeastern boreal forest of Quebec. Canadian Journal of Forest Research 34:

82   353-364.

83   Sirén G. 1955. The development of spruce forest on raw humus sites in northern Finland and its

84   ecology. Acta Forestalia Fennica 62(4).

Supplementary material 2. Field sampling and tree crown size reconstruction

Field sampling

We placed a square grid of 64×64 cells over each of the five studied landscapes with specific criteria: (in order of importance) 1) the entire grid was within an unmanaged forest, 2) the area was accessible by boat or by foot, and 3) the area contained as much forest as possible, given the landscape mosaics. To reduce any systematic bias from the visual interpretation, and to quantify the random error associated with the interpretation, needed to produce the canopy cover posterior distribution, we reconstructed canopy cover for a random sample of the grid cells at the year the aerial photograph was taken. For this, we first divided each grid into quadrants. From each quadrant, we randomly selected cells for field sampling. With the division we ensured that cells were selected from different parts of the landscape, as interpretation error might differ in different parts of the aerial photographs (Wu and Strahler 1994). Except for the two pilot-phase cells sampled in Pommituskukkulat, we only accepted cells located at a minimum distance of 100 m from previously sampled cells.

We located the cells in the field using a consumer-grade GPS (for approximate location) and terrain features visible in the aerial photographs (for accurate location). In each sampled cell, we mapped all trees with a minimum diameter of 10 cm at 1.3-m height, whose crown reached within the cell. We mapped trees using a FieldMap measuring system (IFER ltd., Czech Republic) that utilizes an electronic compass and laser rangefinder (see Aakala and others 2016 for details on the measurements). Dead trees were mapped similarly. Some dead trees had their stem base outside, but close to, the cell border. In such cases, we estimated whether the crown reached within the cell while the tree was alive based on the crowns of nearby live trees of the same species and similar

110 size. For each tree, we recorded diameter at 1.3-m height, species, and tree height. We determined

111 the crown shape of each tree by measuring 4–8 points along the crown perimeter. The exact number

112 of points depended on the irregularity of the crown. We converted these measurements into

113 polygons, describing the crown of each tree.

114

115 **Tree crown size reconstruction**

116

117 Field sampling and the year the aerial photographs were taken were separated by one to two years.

118 We therefore reconstructed the crowns of each tree to correspond to the photography year. For this,

119 we extracted an increment core (from live and standing dead trees) or a partial stem disk (from logs)

120 in the field. Samples were usually extracted between a height of 1 and 1.3 m, but for decayed logs

121 the sample occasionally needed to be taken higher up the stem. We glued the increment core

122 samples to wooden core mounts and sanded them to fine grit (600 for conifers, 1000 for deciduous).

123 Partial stem disks were sanded, or if fragile, first treated in a solution of white glue (as in Krusic

124 and Hornbeck 1989, but in normal air pressure), dried, and sanded. We measured tree-ring widths

125 using the Windendro software (Regents Instruments Ltd.). We visually cross-dated dead trees

126 against a master chronology built from live tree measurements from the same sites, and verified the

127 cross-dating quality, using COFFECHA software (Holmes 1983).

128

129 Using the tree-ring widths, we reconstructed the size difference between the field-measured tree,

130 and the same tree during the year when the aerial photograph was taken. For this, we back-

131 calculated individual tree sizes by first taking the field-measured tree size as a starting point. We

132 then subtracted bark thickness (using species-specific bark thickness equations; Ilvessalo (1965) for

133 all deciduous trees and conifers in Finland, and Li and Weiskittel (2011) for conifers in Quebec),

134 and twice the width of the last ring (for diameter), to calculate diameter under bark of the previous

135   year. We then added bark thickness for the new diameter, and added it to this new diameter. This

136   way we computed tree sizes (over bark) for each tree for each year. If a tree had died during the

137   reconstruction period, it was 'resurrected' at its cross-dated year of death. For downed dead trees

138   the sampling height was sometimes higher than the 1.3-m height. In this case, we relied on the pipe-

139   model assumption that the area of each ring at the sampling height was equal to the area of the same

140   ring at a height of 1.3 m, and converted that area to ring width at a height of 1.3 m (beginning from

141   the field-measured DBH, minus the bark).

142

143   Using species-specific linear regression models between tree diameter and crown area (Figs. S2–

144   S3), we then converted the change in tree size to change in crown size. The crown polygons of each

145   tree were then shrunk using "negative buffering" (rgeos package v.0.3-22 in R; Bivand and Rundel

146   2017), so that polygon shape was assumed to have stayed the same. We assumed circular crowns

147   for trees that died between the field sampling and the year the aerial photo was taken. We calculated

148   the canopy cover for the sampled cells as the sum of non-overlapping areas of crowns within the

149   cell.

150
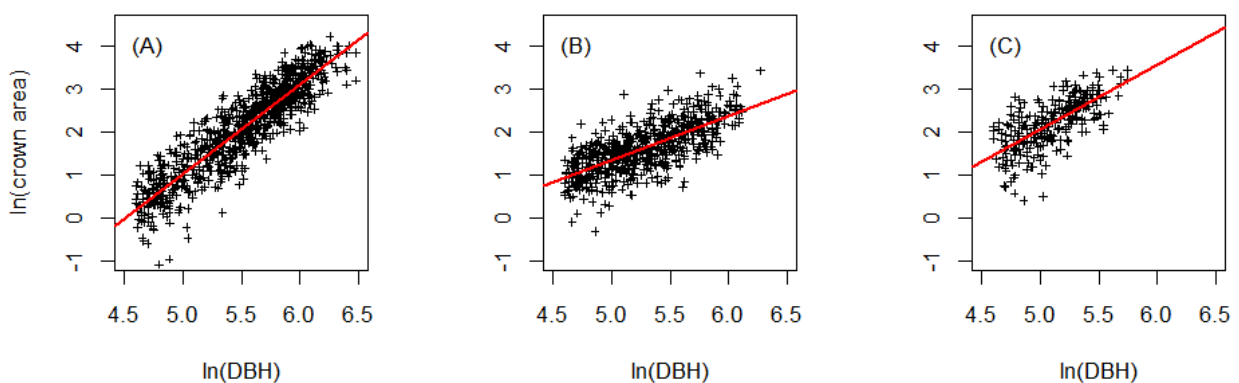
151

152   **Figure S2.** Crown area – tree diameter (DBH, diameter at 1.3-m height) models for northern

153   Finnish Scots pine (A), Norway spruce (B), and pubescent birch (C).
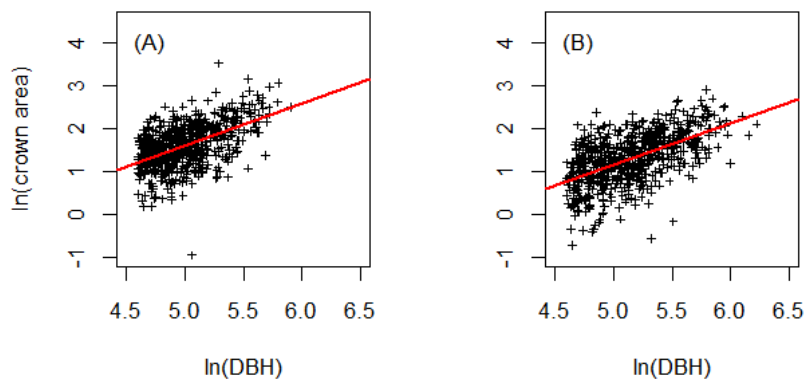
Figure S3. Crown area – tree diameter models (DBH, diameter at 1.3 m height) for eastern

Canadian black spruce (A), and balsam fir (B). For paper birch, models for pubescent birch were

used.

References

Aakala T, Shimatani K, Abe T, Kubota Y, Kuuluvainen T. 2016. Crown asymmetry in high latitude

forests: disentangling the directional effects of tree competition and solar radiation. Oikos 125:

1035-1043.

Bivand R, Rundel C. 2017. rgeos: Interface to Geometry Engine – Open Source (GEOS). R package

version 0.3-22.

De Grandpré L, Morissette J, Gauthier S. 2000. Long-term post-fire changes in the northeastern

boreal forest of Quebec. Journal of Vegetation Science 11: 791-800.

Holmes RL. 1983. Computer-assisted quality control in tree-ring dating and measurement. Tree-

ring Bulletin 43: 51-67.

Ilvessalo Y. 1965. Metsänarvioiminen. WSOY, Porvoo, 400 p. [In Finnish].

Krusic PJ Jr, Hornbeck JW. 1989. Preserving decayed wood samples for tree-ring measurement.

Tree-ring Bulletin 49: 23-27.

173   Li R, Weiskittel AR. 2011. Estimating and predicting bark thickness for seven conifer species in the

174   Acadian region of North America using a mixed-effects modeling approach: a comparison of

175   model forms and subsampling strategies. European Journal of Forest Research 130: 219-233.

176   Wu Y, Strahler AH. 1994. Remote estimation of crown size, stand density, and biomass on the

177   Oregon transect. Ecological Applications 4: 299-312.

178 **Supplementary material 3. Calibration models for visual interpretations, feature**

179 **size approximation, and formation of explanatory variables for canopy cover**

180 **variation**

181

182 **Calibration model formation**

183

184 We calibrated the visual interpretation of canopy cover, and quantified the interpretation error using

185 different regression models between interpreted and reconstructed canopy cover for Finnish and

186 Quebecois landscapes. The calibration model for the Finnish landscapes had more degrees of

187 freedom than the calibration model for the Quebecois landscapes (n = 48, 18, respectively). Hence,

188 we could test the influence of additional variables (tree species proportions, distance from cells to

189 aerial photograph nadirs) for the calibration model for the Finnish landscapes. According to Akaike

190 information criterion for small sample sizes (AICc), the inclusion of the proportion of *P. abies* in

191 the cell as a predictor most improved the calibration model (Table S1).

192

193 **Table S1.** Tested calibration models for the Finnish landscapes. Used predictors were: I_CC =

194 interpreted canopy cover for the cell, P_abies = interpreted proportion of *P. abies* in the cell,

195 P_sylvestris = interpreted proportion of *P. sylvestris* in the cell, B_spp = interpreted proportion of

196 birch species in the cell, D_nadir = average distance from the cell to stereophoto nadirs.

Predictors	R^2	Sigma	AICc
I_CC	0.68	4.41	283
I_CC + P_abies	0.78	3.66	265
I_CC + P_sylvestris	0.74	3.93	275
I_CC + B_spp.	0.68	4.43	285
I_CC + D_nadir	0.68	4.43	283

197 Hence, we included it in the final calibration model for the Finnish landscapes (Fig. S4a). We

198 assessed the model fit and spread with a residual plot, and observed random calibration model

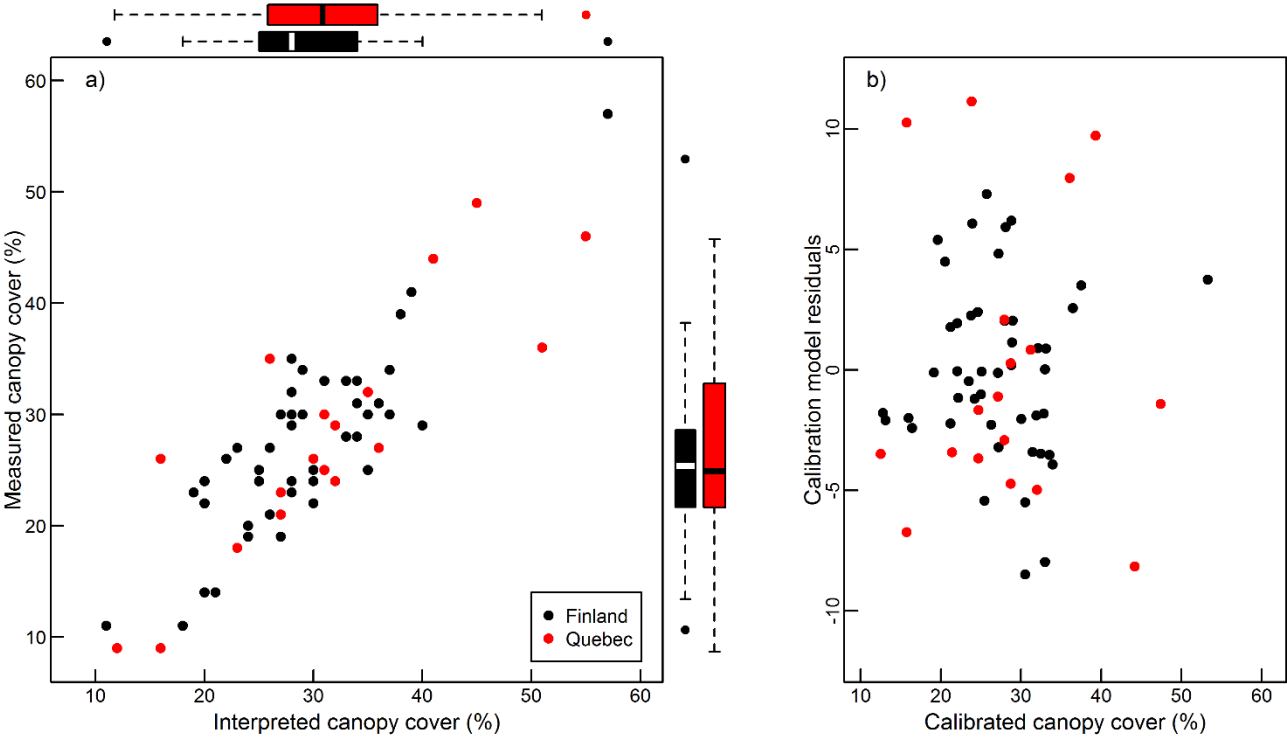199 residual pattern (Fig. S4b).

200

201

Figure S4. The relationship between the interpreted and measured canopy cover and the measured

and interpreted canopy cover distributions (a), and the canopy cover calibration model residuals in

relation to calibrated canopy cover (b). See Table S2 for the posterior means and 95 % highest

posterior density credible intervals for the regression coefficients and error variances.

206

207 Similarly, using different models for different regions, we calibrated the visual interpretation of the

208 summed number of snags and logs in each cell with the equivalent dead wood basal area measured

209 in the field, and compiled the calibration to raster maps (Figs. S5–S6). Dead wood was classified

210 into decay classes in the field measurements (see Aakala 2010 for the decay classes). As decay

211 progresses, the dead stems become less discernible from the forest floor. Hence we tested the

212   cumulative basal area of trees in progressively advanced decay classes as the dependent variable.

213   We observed the best fit for the model when the stems in all but the most advanced decay stages

214   were included. We furthermore assessed the interpretation error sensitivity of the dead wood

215   calibration model in relation to canopy cover. The dead wood calibration model residuals varied

216   randomly in relation to the interpreted canopy cover (Fig. S5b).

217
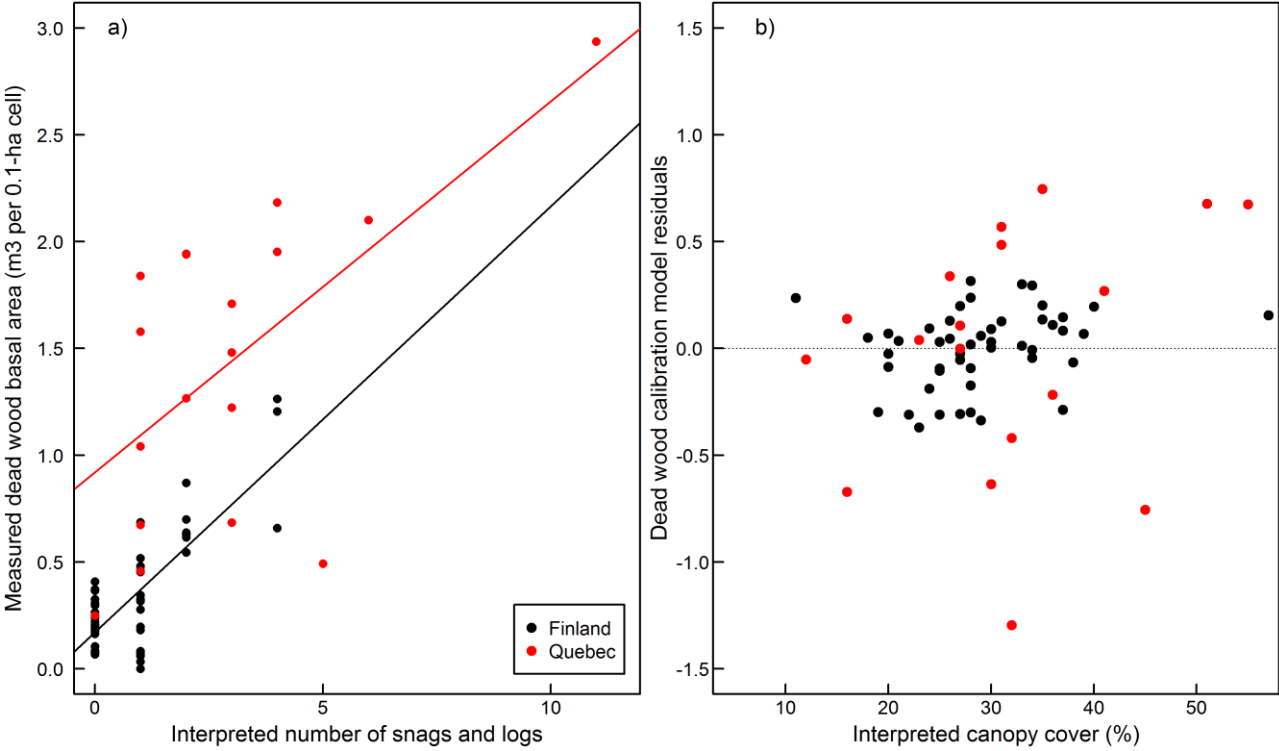
218

219   **Figure S5.** The relationship between the measured dead wood basal area and the interpreted

220   number of snags and logs in the cell, and the fitted calibration models (black line for Finnish and

221   red for Quebecois landscapes) (a), and the dead wood calibration model residuals in relation to

222   interpreted canopy cover (b). See Table S3 for the posterior means and 95 % highest posterior

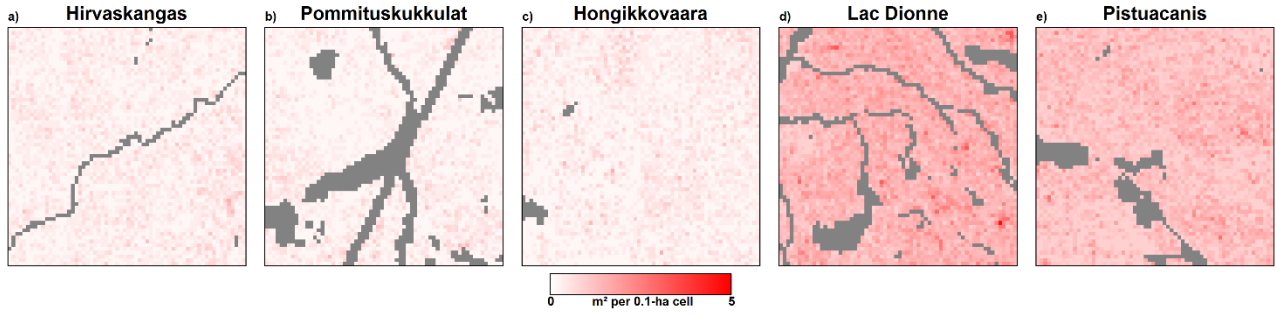223   density credible intervals for the regression coefficients and error variances.

224

Figure S6. The calibrated dead wood basal areas in the studied landscapes.

The following notation is used in the Bayesian calibration models:

y_i^j : canopy cover or the quantity of dead wood reconstructed from field measurements at plot i in country $j = 1,2$, where 1: Finland and 2: Canada.

x_i^j: corresponding visually interpreted canopy cover or dead wood quantity

r_i: relative canopy cover of *P.abies* in Finnish plots.

The sample sizes in Finnish and Canadian sites are, $n_1 = 48$, $n_2 = 18$, respectively.

In vector form:

$$Y^j = \left[y_1^j, \dots, y_{n_j}^j \right]^T,$$

$$X^j = \left[x_1^j, \dots, x_{n_j}^j \right]^T,$$

$$R = \left[r_1, \dots, r_{n_1} \right]^T.$$

Lets denote by J^j a $n_j \times 1$ column vector of ones.

The linear regression model is then:

$$Y = X\beta + \epsilon,$$

where $\epsilon \sim N(0, \sigma^2 I)$ and in the case of Finnish canopy cover

244    $Y = Y^1$, $X = [J^1, X^1, R]$, $\beta = [\beta_0, \beta_1, \beta_2]^T$, and , $I = n_1 \times n_1$ identity matrix,

245   and for Canadian canopy cover and for the dead wood models for both countries

246    $Y = Y^2$, $X = [J^2, X^2]$, $\beta = [\beta_0, \beta_1]^T$, and , $I = n_2 \times n_2$ identity matrix.

247

248   We use an uninformative prior for the unknown parameters β and σ^2,

249    $$p(\beta, \sigma^2 | X) \propto \sigma^{-2}.$$

250

251   In this model the marginal posterior distribution of the regression coefficients is a multivariate t-

252   distribution with v degrees of freedom, where $v = n - 3$ for canopy cover in Finland and $v = n -$

253   2 for other cases (see e.g., Gelman and others 2004):

254

255    $$\beta | Y, X \sim t_v \left(\hat{\beta}, s^2 V_\beta \right),$$

256   where

257    $$\hat{\beta} = (X^T X)^{-1} X^T Y,$$

258

259    $$V_\beta = (X^T X)^{-1},$$

260   and

261    $$s^2 = \frac{1}{v} \left(Y - X\hat{\beta} \right)^T \left(Y - X\hat{\beta} \right).$$

262   The marginal posterior distribution for the noise variance is

263    $$\sigma^2 | Y, X \sim Inv - \chi^2(v, s^2).$$

264

265 Last, we extracted the posterior means and 95% highest posterior density credible intervals for the

266 regression coefficients and error variance for the canopy cover and dead wood calibration models

267 (Tables S2–S3, respectively).

268

269 **Table S2.** The posterior means and 95% highest posterior density credible intervals for the

270 regression coefficients and error variance for the canopy cover calibration model.

		Posterior mean	Credible interval
Finland	β_0	5.20	[0.63, 9.75]
	β_1	0.84	[0.70, 0.99]
	β_2	-7.59	[-10.88, -4.27]
	σ^2	14.00	[8.60, 20.15]
Canada	β_0	2.74	[-6.46, 11.89]
	β_1	0.81	[0.54, 1.09]
	σ^2	43.09	[17.59, 77.37]

271

272 **Table S3.** The posterior means and 95% highest posterior density credible intervals for the

273 regression coefficients and error variance for the dead wood calibration model.

		Posterior mean	Credible interval
Finland	β_0	0.17	[0.10, 0.24]
	β_1	0.20	[0.15, 0.25]
	σ^2	0.036	[0.022, 0.051]
Canada	β_0	0.92	[0.46, 1.38]
	β_1	0.17	[0.06, 0.29]
	σ^2	0.40	[0.16, 0.72]

274

Consideration of calibration success

276

277 To reduce bias due to improving interpretation skill and accuracy, we interpreted the aerial

278 photographs in randomized order. Still, the calibrated canopy cover maps showed traces of the sub-

279 grids used in the interpretation. In certain landscapes, especially Hirvaskangas, the relative canopy

280 cover maps also still held these traces. While our inability to remove the interpretation bias

281 definitely weakens our data, the low canopy cover interpretation error (calibration model sigma 3.7

282 for Finland, 6.1 for Quebec) indicated that the data were of adequate quality and suitable for the

283 performed analyses.

284

285 We noted that the proportion of *P. abies* was negatively related to mid- and large-scale relative

286 canopy cover especially in Pommituskukkulat landscape. Because the proportion of *P. abies* was

287 also used in the calibration model, we tested whether the relation could be detected if the

288 interpretation were calibrated without the proportion of *P. abies*. The negative relative canopy cover

289 still occurred at areas with high proportion of *P. abies*, and was hence independent of the used

290 calibration model.

291

Posterior predictive distribution for the calibration models

293

294 We used Bayesian inference as follows, to distinguish credible variation in relative canopy cover

295 from noise due to the error in the visual interpretation. Let us denote the matrix of explanatory

296 variables in the whole vectorized 64×64 grid of a given area by $\tilde{X}$, where $= [\tilde{J}, \tilde{X}_1, \tilde{R}]$ for canopy

297 cover in Finland and $\tilde{X} = [\tilde{J}, \tilde{X}_2]$ for dead wood and canopy cover in Canada, where $\tilde{J}$ is a 4096

298 column vector of ones. The calibrated canopy cover or dead wood corresponding to $\tilde{X}$ is then $\tilde{X}\beta$.

299 However, as the regression coefficients are in fact random variables, also the calibrated variable is a

300 random variable and has the posterior distribution $p(\tilde{X}\beta|Y,X,\tilde{X})$ with mean $\tilde{X}\hat{\beta}$. However, the

301 variation in such a posterior reflects only the uncertainty in the regression coefficients and neglects

302 the variation in the calibrated values caused by the deviations from the regression plane. Therefore,

303 we model the calibrated variable as

304

305 $$\tilde{Y} = \tilde{X}\beta + \epsilon,$$

306

307 where $\epsilon \sim N(0, \sigma^2 I)$, where I is the 4096×4096 identity matrix. The distribution of $\tilde{Y}|Y,X,\tilde{X}$ is

308 referred to as the posterior predictive distribution and it is given by:

309

310 $$\tilde{Y}|Y,X,\tilde{X} \sim t_\nu \left(\tilde{X}\hat{\beta}, s^2 \left(I + \tilde{X}V_\beta\tilde{X}^T \right) \right).$$

311

312 (see e.g., Gelman and others 2004 for details). Only a few cells in the Quebecois landscapes

313 credibly deviated from their surroundings, while the Finnish landscapes held a greater number of

314 credible cells. There are two reasons for this. First, the fewer field measurements in Quebecois

315 landscapes led to smaller degrees of freedom in the posterior distribution. Secondly, the estimated

316 standard deviation was somewhat larger in Quebec.

317

318 Zero snags and logs were interpreted in many grid cells. Hence, the dead wood posterior predictive

319 samples could have had plenty of negative draws (negative dead wood basal area). We quantified

320 the amount of the cells with such negative draws. We noted that app. 7 % of the 0.1-ha cells in

321 Quebecois landscapes and app. 20 % in the Finnish landscapes had negative draws in the dead

322 wood posterior predictive samples. In Quebec, these cells (cells which had negative draws in the

323 posterior predictive samples), the majority had less than 5 % negative draws of the total 10 000

324   samples drawn. Here, we assumed that the small quantity of negative samples did not affect the

325   interpretation of the results. In Finland, app. 60 % of the cells had less than 5 % negative draws in

326   the 10 000 samples, and the rest 40 % had roughly 20 % negative draws in the samples. We tested

327   the influence of the negative samples to the results by replacing all the draws in the samples with

328   zero. Truncation of the negative values did not affect the conclusions drawn from the analyses.

329

330   **Estimating feature size of the extracted components**

331

332   We evaluated the multimodality of the scale-derivative norms by drawing them for each extracted

333   component and expected one peak in the norm. The unimodality of the scale-derivative norms

334   confirmed a successful extraction (Fig. 3). To extract the spatial scales at which the most salient

335   forest structural features occur, some scale breaks needed to be manually placed. Hence, we verified

336   the existence of all identified and extracted scales by comparing the scale-derivative norm of the

337   canopy cover (sum of all scale-dependent components) to the scale-derivative norm of the permuted

338   canopy cover (Fig. S7). Only the small-scale component could be identified from the permuted

339   data, confirming the existence of the identified characteristic scales of variation.
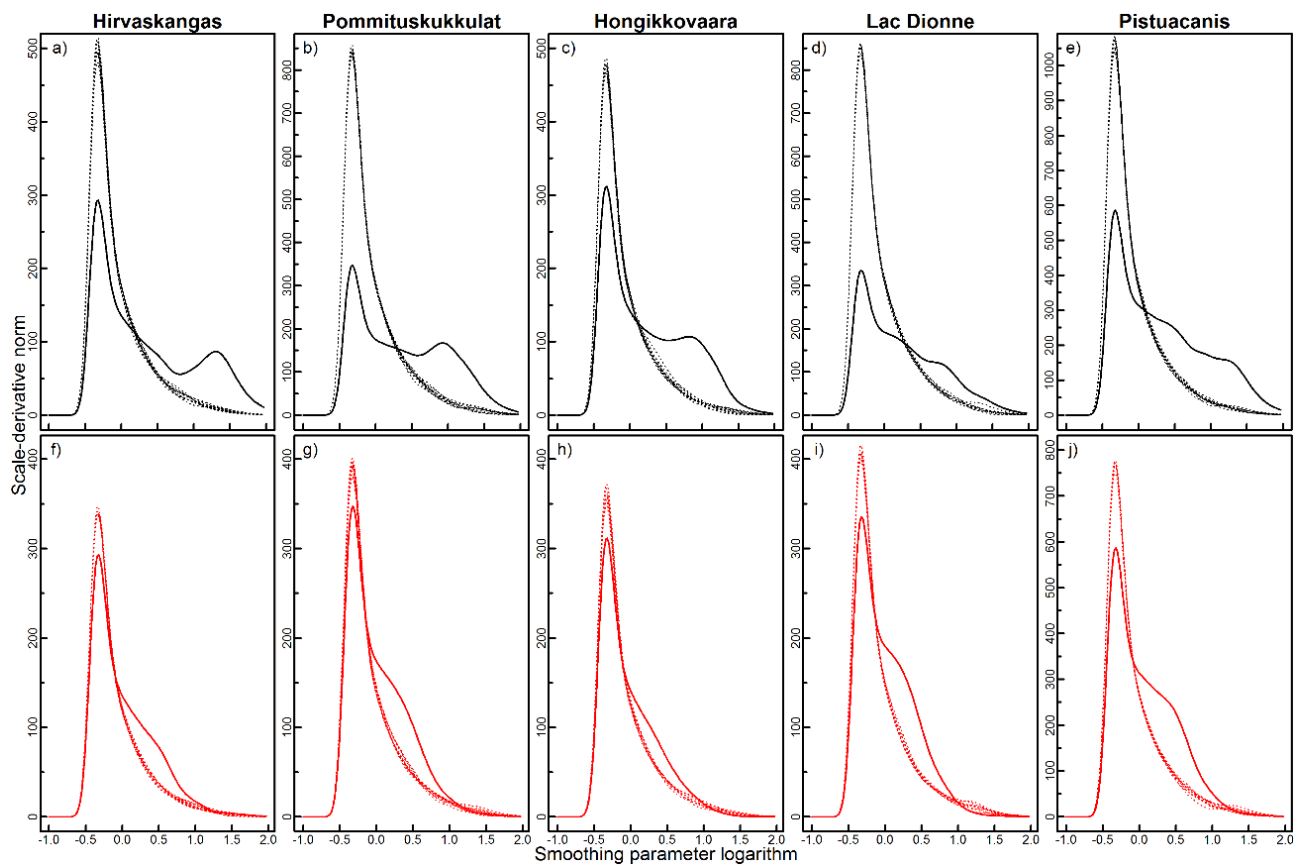
340

Figure S7. The comparison of the scale-derivative norms and the corresponding permuted norms. In the top row (a-e) the solid black line indicates scale-derivative norm for calibrated canopy cover (sum of all scale-dependent components (small-, mid- and large-scale), and the dashed black lines represent 10 instances of the scale-derivative norms for permuted calibrated canopy cover. In the bottom row (f-j) the solid red line indicates the scale-derivative norm for the sum of small- and mid-scale components, and the dashed red lines represent 10 instances of the scale-derivative norms for permuted sum of corresponding components.

To approximate the spatial scales of variation, we assessed patch sizes in the relative canopy cover maps as the diameter of a representative circle. A representative diameter of a circular patch in the extracted component can be estimated using the effective range of a smoother with a smoothing level indicated by the location of the peak in the component's scale-derivative norm (Pasanen and others 2018). The range spans from the signal's minimum value to a new minimum, or from a

355 maximum to a new maximum, hence covering both positive and negative intensities. However, here

356 a feature is considered to be a patch with a similar relative canopy cover (i.e. either positive or

357 negative intensity). The diameter of a feature is therefore given as the diameter of a circle where the

358 smooth of an impulse response has dropped below half of its maximum value. The approach

359 corresponds to the concept of full width at half maximum, which is often used e.g. in medical

360 imaging to represent the size of a feature that has no clear boundaries (Epstein 2007).

361

362 **The formation of explanatory variables for canopy cover variation**

363

364 To analyze the relationship between variation in relative canopy cover and dead wood quantity, we

365 extracted scale-dependent features of the dead wood basal area, using the same smoothing levels as

366 with canopy cover (Fig. S8).

367

368 To assess the influence of stand age and soil productivity, we used existing understanding of how

369 tree species compositions reflect site productivity and past disturbances for both study regions,

370 based on the fairly predictable variability in species composition with site type and with stand

371 successional development. In Quebec, poorer sites are dominated by *P. mariana*, whereas the

372 proportion of *A. balsamea* increases at more productive mesic sites (De Grandpré and others 2000).

373 In Finland, *P. sylvestris* dominates xeric sites, while the more productive mesic sites usually follow

374 a successional change from *Betula* spp. dominance early in the succession to *P. abies* dominance in

375 the late-successional state (Sirén 1955). On sub-xeric sites of average productivity, the absence of

376 fire leads to an increasing share of *P. abies* over the long term.

377

378 For Quebecois landscapes, we utilized tree species composition maps created by the Ministère des

379 Forêts, de la Faune et des Parcs du Québec, based on aerial photointerpretation of experienced

380   interpreters. We classified the study areas into polygons of either pure *P. mariana*, *A. balsamea*, or

381   deciduous dominance or their mixtures. We lacked such independent tree species composition maps

382   for Finnish landscapes. Hence we obtained tree species compositions from visual interpretation of

383   the aerial photographs, and field measurements. Similar to total canopy cover and dead wood, we

384   used linear regression models to calibrate the visual interpretations of *P. sylvestris, P. abies*, and the

385   deciduous tree canopy cover proportions with field measurements (Fig. S9). We converted the cells

386   into polygons, classified them as pure stands or mixtures (pure stand if individual species had

387   canopy cover proportion $> 75\%$), and smoothed the polygons (Fig. S10). For comparison we further

388   simplified the polygons according to the dominant species (Fig. S11). We visually compared the

389   credible relative canopy cover and tree species compositions of the study landscapes.
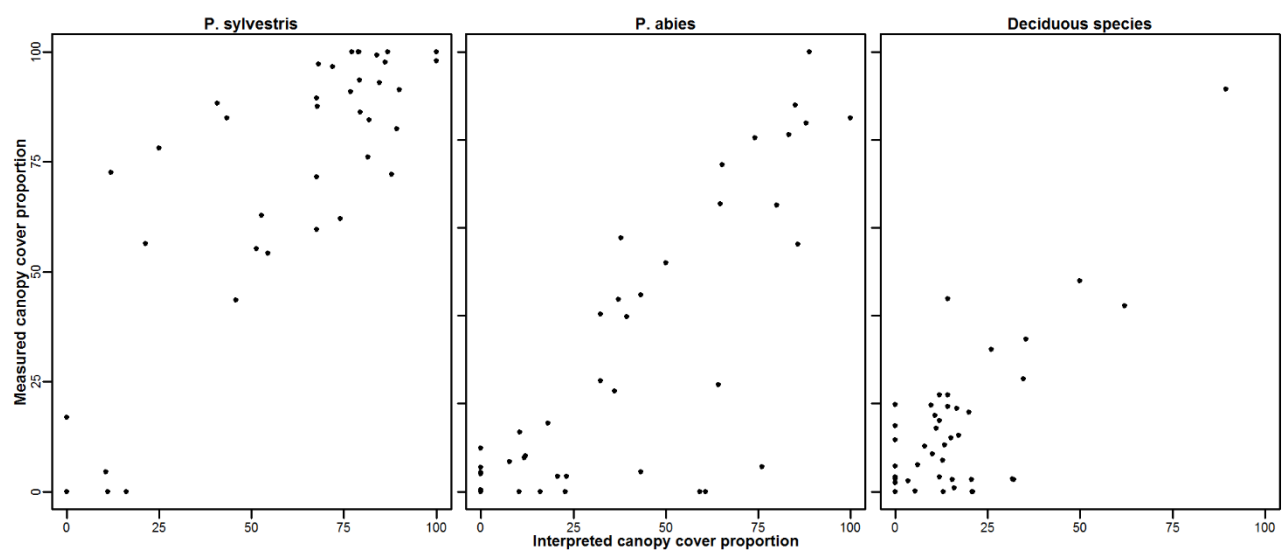
390

391
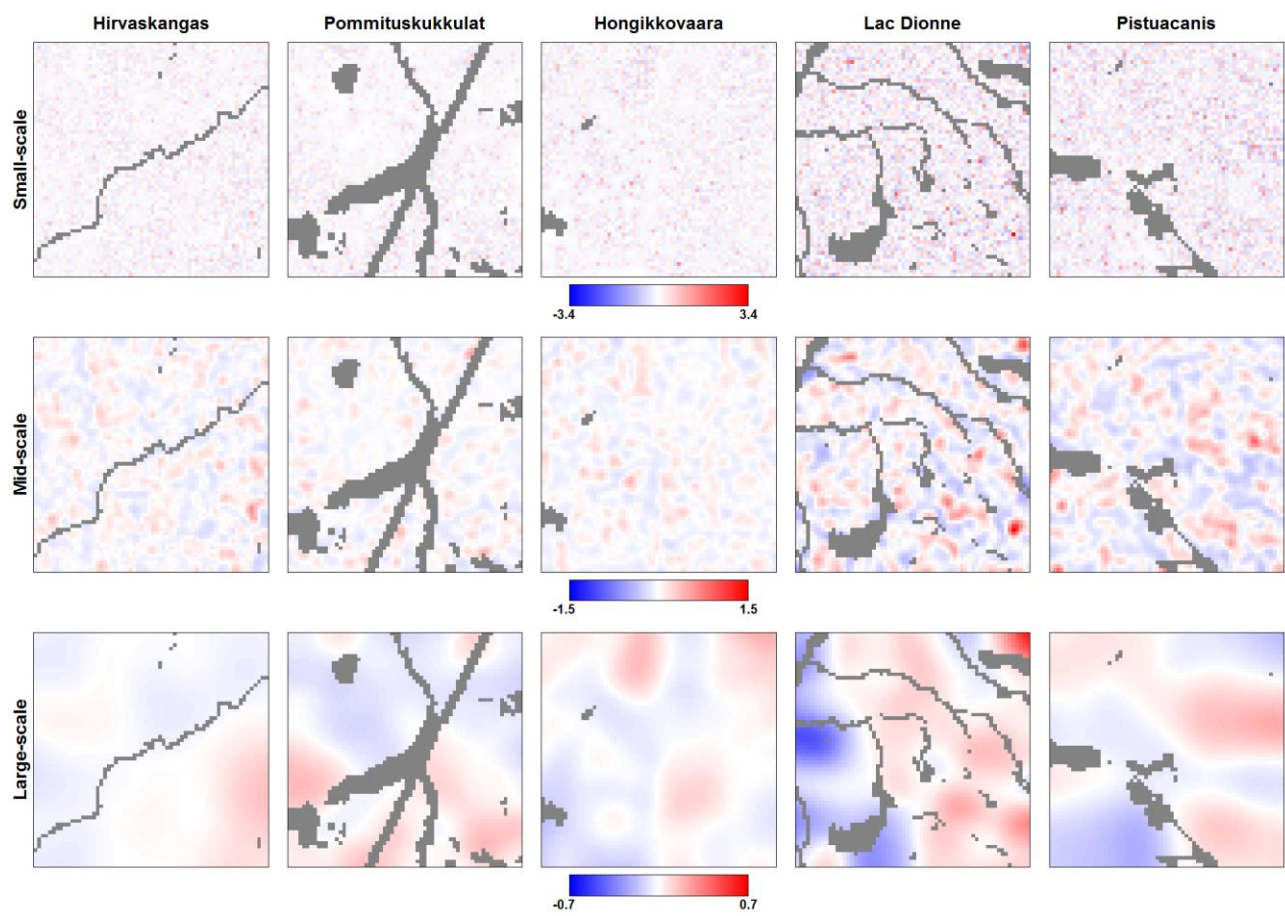
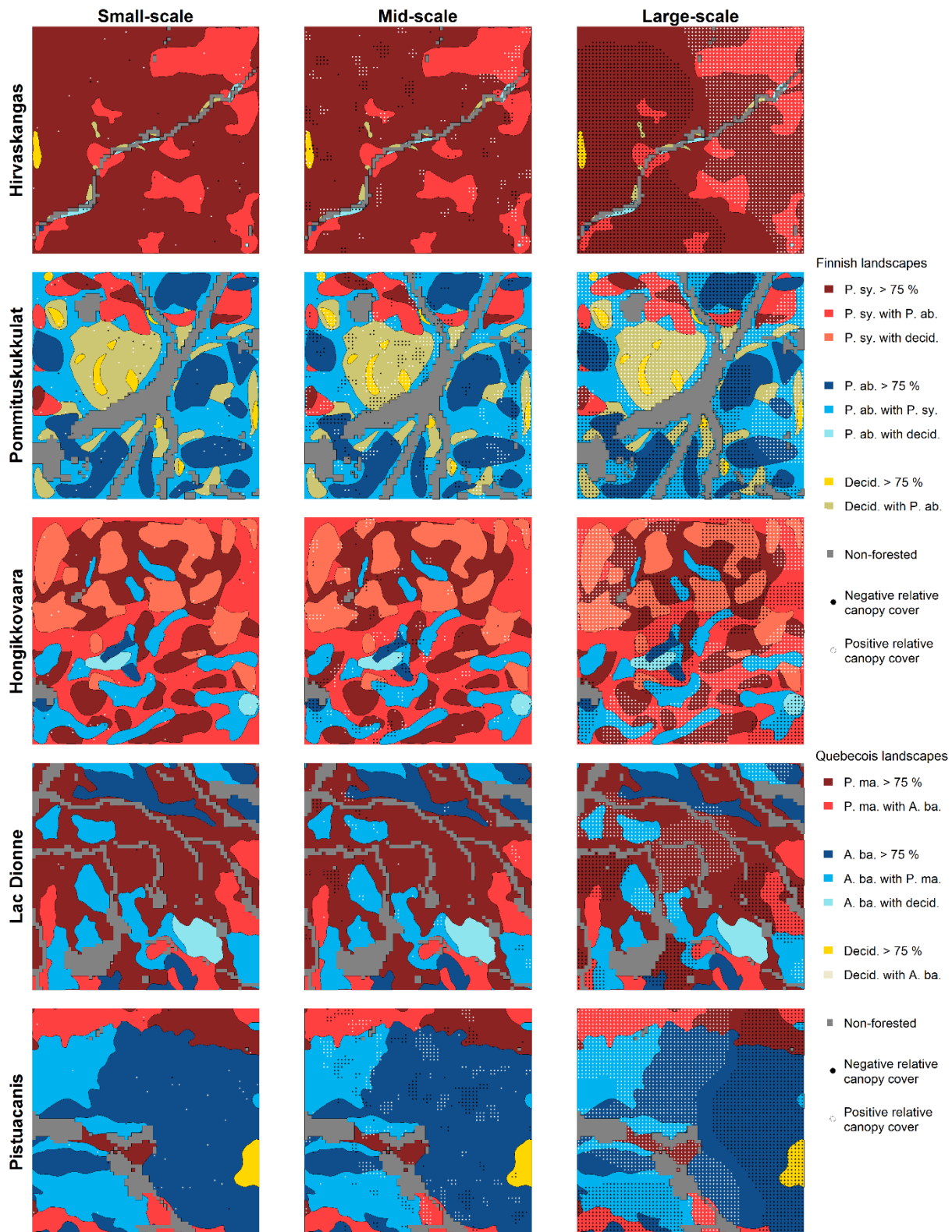**Figure S8.** Relative dead wood basal areas in the study landscapes at multiple spatial scales.

393

394

Figure S9. The relationship between the interpreted and measured tree species canopy cover

proportions in the Finnish landscapes.

Figure S10. Tree species compositions and credible relative canopy covers in the study landscapes.

P. sy. = *Pinus sylvestris,* P. ab. = *Picea abies*, P. ma = *Picea mariana,* A. ba. = *Abies balsamea*,
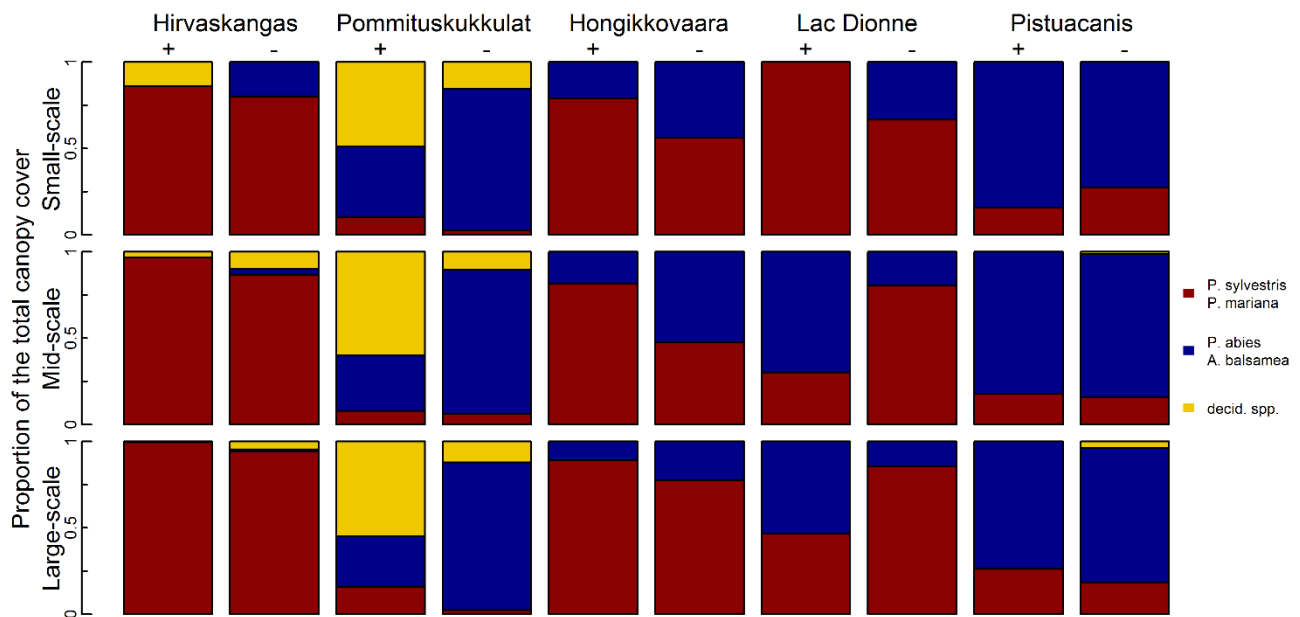
decid. = deciduous species.

Figure S11. Tree species proportions of the total canopy cover in cells with credible positive (+) or negative (-) relative canopy cover. P. sylvestris and P. abies are present in Hirvaskangas, Pommituskukkulat and Hongikkovaara, P. mariana and A. balsamea in Lac Dionne and Pistuacanis.

References

Aakala T. 2010. Coarse woody debris in late-successional *Picea abies* forests in northern Europe: variability in quantities and models of decay class dynamics. Forest Ecology and Management 260: 770-779.

De Grandpré L, Morissette J, Gauthier S. 2000. Long-term post-fire changes in the northeastern boreal forest of Quebec. Journal of Vegetation Science 11: 791-800.

Epstein CL. 2007. *Introduction to the mathematics of medical imaging*. Society for Industrial and Applied Mathematics. 84p.

Gelman A, Carlin JB, Stern HS, Rubin DB. 2004. Bayesian Data Analysis. Second edition. Chapman and Hall/CRC.

417   Pasanen L, Aakala T, Holmström L. 2018. A scale space approach for estimating the characteristic

418   feature sizes in hierarchical signals. Stat, in press.

419   Sirén G. 1955. The development of spruce forest on raw humus sites in northern Finland and its

420   ecology. Acta Forestalia Fennica 62(4).